




Review

Bacteriophage Tail Proteins as a Tool for Bacterial Pathogen Recognition—A Literature Review

Karolina Filik ^{*}, Bożena Szermer-Olearnik ^{*}, Sabina Oleksy, Jan Brykała and Ewa Brzozowska 

Hirszfeld Institute of Immunology and Experimental Therapy, Polish Academy of Sciences, St. R. Weigl 12, 51-167 Wrocław, Poland; oleksy.sabina01@gmail.com (S.O.); janbrykala@gmail.com (J.B.); ewa.brzozowska@hirszfeld.pl (E.B.)

* Correspondence: karolina.filik@hirszfeld.pl (K.F.); bozena.szermer-olearnik@hirszfeld.pl (B.S.-O.)

Abstract: In recent years, a number of bacterial detection methods have been developed to replace time-consuming culture methods. One interesting approach is to mobilize the ability of phage tail proteins to recognize and bind to bacterial hosts. In this paper, the authors provide an overview of the current methodologies in which phage proteins play major roles in detecting pathogenic bacteria. Authors focus on proteins capable of recognizing highly pathogenic strains, such as *Acinetobacter baumannii*, *Campylobacter* spp., *Yersinia pestis*, *Pseudomonas aeruginosa*, *Listeria monocytogenes*, *Staphylococcus aureus*, *Enterococcus* spp., *Salmonella* spp., and *Shigella*. These pathogens may be diagnosed by capture-based detection methods involving the use of phage protein-coated nanoparticles, ELISA (enzyme-linked immunosorbent assay)-based methods, or biosensors. The reviewed studies show that phage proteins are becoming an important diagnostic tool due to the discovery of new phages and the increasing knowledge of understanding the specificity and functions of phage tail proteins.

Keywords: RBP; tail fiber protein; pathogens detection; bacteriophages; diagnostic



Citation: Filik, K.; Szermer-Olearnik, B.; Oleksy, S.; Brykała, J.; Brzozowska, E. Bacteriophage Tail Proteins as a Tool for Bacterial Pathogen Recognition—A Literature Review. *Antibiotics* **2022**, *11*, 555. <https://doi.org/10.3390/antibiotics11050555>

Academic Editors: Carla M. Carvalho and Marc Maresca

Received: 2 March 2022

Accepted: 19 April 2022

Published: 21 April 2022

Publisher's Note: MDPI stays neutral with regard to jurisdictional claims in published maps and institutional affiliations.



Copyright: © 2022 by the authors. Licensee MDPI, Basel, Switzerland. This article is an open access article distributed under the terms and conditions of the Creative Commons Attribution (CC BY) license (<https://creativecommons.org/licenses/by/4.0/>).

1. Introduction

Bacteriophages represent the most abundant life form on Earth and can be found in all environments in which bacteria grow. Phages are detected in ground and surface water, soil, food, sewage, as a component of human and animal microbiomes, etc. [1]. They are responsible for 10–80% of the total bacterial mortality in aquatic ecosystems and are an important factor limiting bacterial populations [2,3]. A characteristic feature of bacteriophages is their affinity for specific bacteria, which arises through their ability to specifically recognize molecules present on the host bacterial surface. This property has been successfully used for bacterial diagnosis and identification [4]. The interactions between phages and their hosts depend on the phage morphology, bacterial surface structures, and environment. The so-called monovalent bacteriophages infect a specific strain of bacteria, while the polyvalent bacteriophages show specificity towards several bacterial strains [5]. The specific molecules through which bacteriophages bind to the bacterial cell surface include lipopolysaccharide (LPS), fimbriae, flagella, and various proteins [6]. Bacteriophages that infect encapsulated bacteria need to break down the capsule barrier to reach their cell-surface receptor. These phages bind to polysaccharides of the capsule and mimic an enzyme-substrate reaction to degrade the cell envelope. Some bacteriophage-generated enzymes diffuse into the medium, strip the cell sheaths from around the plaques, and induce a “halo” zone [7]. The degrading enzymes may be part of the phage tail, such as the tail tubular proteins (TTP) [8,9]. The varied structural composition of the bacterial cell surface means that there is a wide range of molecules that can act as receptors. On Gram-positive bacteria, potential recognition roles are played by cell wall elements such as teichoic acids and lipoteichoic acids; on Gram-negative bacteria, the targeting molecules include LPS, outer membrane proteins (e.g., porins), pili, and flagella [6,10]. Kinetically, the adsorption process is a first-order reaction whose rate is directly proportional to the concentrations of both phage and

bacteria. In an environment where phages dominate, even several hundred phage particles can adsorb on a single host cell [11]. The adsorption constant can be calculated theoretically as a function of the virus diffusion rate (as a factor leading to virus-cell collision), virus dimensions, environmental viscosity, and environmental temperature [12].

Prior to phage adsorption, the bacterial cell surface must be modified through the involvement of cations and (in some cases) the attachment of tryptophan or another cofactor, such as phenylalanine, tyrosine, or diiodotyrosine. Some agents, such as 2-pyridylalanine and 3-pyridylalanine, facilitate the adsorption of the phage to the bacteria [13]. The presence of electrolytes in the culture medium both supports the adsorption of phage particles to bacteria and influences the effective infection of host cell [13,14]. The presence of calcium, magnesium, and barium ions may inhibit the activity of some phages, while others seem to require calcium ions for virus adsorption [15]. In the absence of electrolytes, adsorption can be reversible and non-infective. Low-molecular-weight organic compounds can attach to and activate phage particles. For example, six tryptophan molecules are necessary to activate bacteriophage T4 [16]. Indole, on the other hand, inhibits the adsorption of a bacteriophage to the bacterial cell. Organic compounds may alter the conformation of sites responsible for the bacterial cell binding of a phage, thereby facilitating or preventing adsorption [17].

Tailed phages of order *Caudovirales* can be classified into three groups on the basis of their tail structures (Figure 1), which relate to the structures of their target capsids. Phages having a short, non-contractile tail are classified as *Podoviridae*; phages with a contractile tail are classified as *Myoviridae*; and those with a long but non-contractile tail are classified as *Siphoviridae* [10,18].

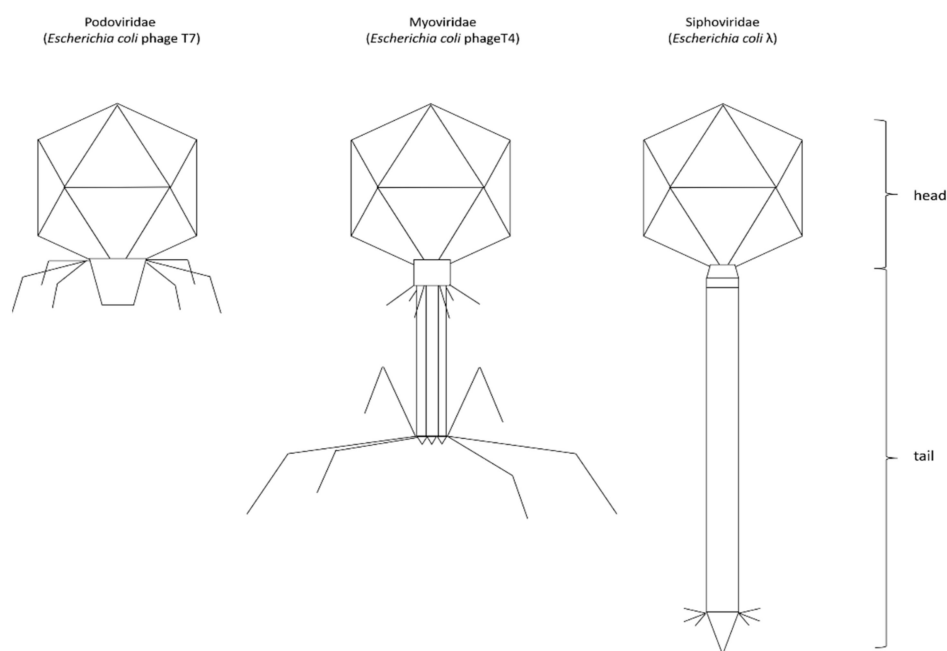


Figure 1. Classification of the *Caudovirales* based on the tail structure.

Phage tails show high specificity and fulfill key tasks to enable phage infection. The phage tail and its RBP (receptor binding proteins) critically govern host recognition via the specific interaction between attachment sites of the tail and molecules on the bacterial surface. To recognize receptors on the surface of bacterial cells, tailed phages use either a set of tail fibers (TF; there may be 3, 6 or 12 fibers) or a single TF located in the center of the baseplate. The adsorption of RBPs to specific bacterial surface molecules is reversible at the beginning and turns into irreversible interaction [10]. The model phage of *Podoviridae* is *Escherichia coli* phage T7. One vertex of its icosahedron capsid protein, gp8, forms a portal that contributes to DNA transport and also acts as a connector for the tail. The tail

comprises six molecules of gp12 and 12–18 copies of gp11. The tail fibers are localized on the tail just below where it joins with the capsid. The phage has six tail fibers, each of which comprises a gp17 trimer [19]. One of the most extensively studied model phages is the T4 bacteriophage, which belongs to the *Myoviridae* family. The T4 tail has the most complex morphology among the Caudovirales. Structurally, the tail is attached to the head by the collar, which sprouts six whiskers. These whiskers are encoded by the gene *wac* (whisker antigen control); they comprise fibrin protein, which plays a crucial role in correct tail assembly during the final phase of phage infection. Fibrin moieties attach to the head of the fiberless phage and form the collar. The whiskers interact with the LTF (long tail fibers), stimulating the assembly and attachment of the LTF to the baseplate [20]. The next part of the tail is the tube, which consists of an internal tube (gp19) and a sheath that is built around the internal tube from gp18 subunits [21,22]. At the distal part of the tube is a baseplate with attached LTF [22,23]. The baseplate consists of gp9, gp10, gp11, and gp12. The long tail fiber consists of gp34, gp35, gp36, and gp37. In T4 phage, the long tail fibers take part in host recognition through a reversible interaction of their tips with LPS or porin. The whiskers (also called short tail fibers) are responsible for an irreversible interaction: upon receptor binding, a recognition signal sent to the baseplate causes the whiskers to extend and bind to the core region of LPS [24]. The model phage of *Siphoviridae* is *E. coli* phage λ , which has a long tail that consists of a tube made from gpV. The major role of the tube is DNA transport and injection during infection. At the distal part of the tube, there is a single tail fiber composed of gpJ. The fiber facilitates the attachment of phage λ to the host cell by binding to LamB on the bacterial envelope surface [25].

Once successful binding to the host receptor has occurred, a conformational alteration in the phage's baseplate takes place, leading to sheath contraction and injection of the phage's nucleic acids into the host cell [6]. The RBPs include phage tailspike, tail fiber, and spike proteins. Due to their diverse host-binding specificities, RBP-encoding genes are often missed by genomic sequence analyses based solely on homology with known RBPs. Even if phage RBPs share structural homology, they tend to lack sequence homology. RBPs have been shown to be very stable proteins with high resistance to proteases and detergents [26]. Overall, the high stability, specificity, and ease of recombinant overexpression make RBPs excellent alternatives to antibodies and ideal tools for the development of new diagnostic technologies.

2. Overview of Methodologies That Use Bacteriophage Tail Proteins for Detecting Pathogenic Bacteria

For diagnostic applications, whole phages and phage-derived proteins have been extensively explored [27]. According to Meile et al. (2020), phage-based pathogen recognition tools can be divided into two categories by their modes of action: infection-based and capture-based detection methods (Figure 2). In the present review, we focus on capture-based detection methods in which tail proteins are used as bio-sensing molecules to detect a particular bacterial strain. In the following, we describe the relevant methodologies that may be implemented for bacterial detection.

Whole phage particles can be applied as bio-recognition elements through their specific binding to the host. This approach has been extensively explored in the development of biosensors. A biosensor can be defined as a detection device in which biomolecular interactions between a bioprobe and an analyte are translated into a measurable signal by means of transduction systems [28]. A typical biosensor consists of a surface functionalized with a biorecognition element, a transduction system that generates a signal reflecting the number of binding events, and an amplifier that processes the signal to give a readable output [29]. The bioprobe is arguably the most crucial element: it confers specificity and sensitivity, which are essential features of a reliable diagnostic tool. Various types of molecules have been used for this purpose, including nucleic acids [30], antibodies or antibody fragments [31,32], and both wild-type and engineered phages (reporter phages) [33]. Another group of potential bioprobes comprises phage-derived binders, such as RBP (described

in more detail below) [34,35], endolysin cell wall-binding domains (CBD) [36–38], and phage-display peptides [39,40]. Details may be found in existing comprehensive reviews of biosensor transduction systems and their modes of action, e.g., [41].

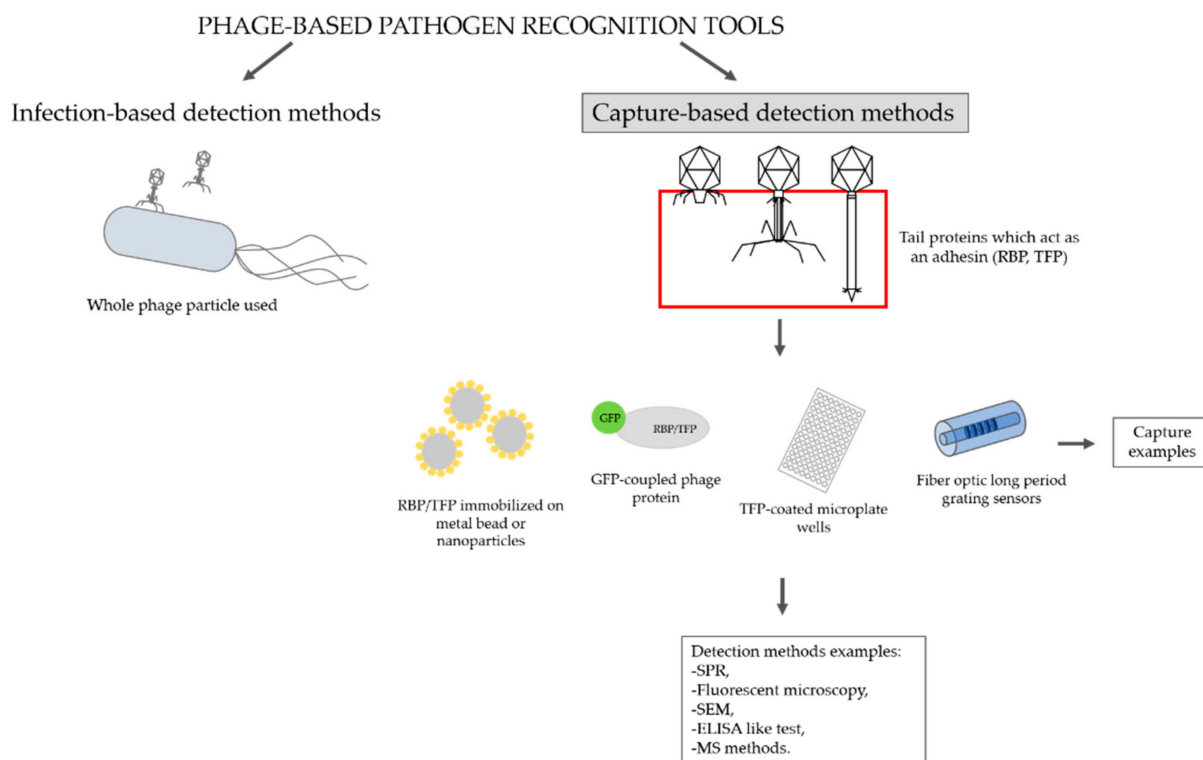


Figure 2. Phage-based pathogen recognition tools. SPR—surface plasmon resonance; SEM—scanning electron microscopy; ELISA—enzyme-linked immunosorbent assay; MS—mass spectrometry.

In addition to surface-immobilized phages in biosensors, whole phage particles, conjugated with, e.g., magnetic nanobeads can also be used as capture probes in bacterial detection assays. However, the large size and possible lytic properties of whole phages may complicate such efforts [42]. Accordingly, researchers have sought to apply phage-derived affinity molecules, such as tail fiber or tailspike RBP and some endolysin CBD. As there are considerable differences in the cell envelopes of Gram-negative and Gram-positive bacteria, it is no wonder that the cell wall-targeting endolysins evolved different structures: phages that infect Gram-positive hosts possess endolysins with both an enzymatically active domain (EAD) and a CBD, whereas those that infect Gram-negative bacteria have endolysins in the dominant majority consisting of a single EAD [43]. CBD are believed to specifically recognize peptidoglycan modifications and decorations, which are characteristic of and common in Gram-positive bacteria [44–47]. However, due to the conserved nature of peptidoglycan, the mechanisms of enzymatic cleavage are much more limited; only five classes of endolysins have been described to date [48]. The above has several implications for the application of endolysin for bacterial detection: (1) only endolysins from phages of Gram-positive hosts can be readily used for bacterial detection and, conversely, only Gram-positive bacteria can be detected with this approach; (2) the separation of the recognition element and enzymatic activity facilitates the development of a single domain into a bioprobe; and (3) the high specificity of recognition by CBD yields a desirably narrow host range. The feasibility of CBD-based pathogen recognition has been reported by multiple research groups. For instance, endolysin CBD fused with fluorescent proteins have been applied as labeling probes in fluorescence microscopy [49–52]. CBD has been coated onto magnetic beads for the separation and enrichment of bacteria, followed by culture-based enumeration [53,54], polymerase chain reaction (PCR)-based detection [53], the use of reporter phage [55], commercial ATP bioluminescence assays [56], or staining

with fluorescently labeled CBD [49]. The development of a lateral flow assay (strip test) employing fusion proteins of an endolysin CBD to detect *Bacillus cereus* has also been reported [57]. Table 1 summarizes the methodologies in which phage tail proteins have been used to detect host bacteria.

Table 1. Overview of methods based on RBP or TFP from different bacteriophages.

Target Species	Capture Method	Detection (Visualization) Method	Limit of Detection	Reference
<i>Acinetobacter baumannii</i>	Sandwich fluorescence assay	Fluorescence (FITC-labeled probes)	6.2×10^2 CFU/mL	[58]
	Magnetic beads coated with TFP	Bioluminescence (ATP release with luciferin/luciferase detection)		
	Magnetic nanoparticles coated with TFP	MALDI-TOF MS	$\sim 2.34 \times 10^5$ and $\sim 4.48 \times 10^4$ CFU/mL, depending on the strain	[59]
<i>Acinetobacter baumannii</i> Pse + other Pse bacteria (Pse-Ppseudomonas acid)	Incubation in solution	Fluorescently labeled probe	-	[60]
	TFP-coated microplate wells	FITC labeling of bacteria		
<i>Enterococcus faecalis</i> , <i>Enterococcus faecium</i>	Magnetic nanoparticles coated with His-tagged TFP	Array of spin-valve sensors on the biochip	10 CFU/mL	[61]
<i>Staphylococcus aureus</i>				
<i>Pseudomonas aeruginosa</i>	Magnetic particles	Magnetic separation	6.7×10^2 CFU/mL and 1.7×10^2 CFU/mL	[62]
	Fluorescent labeling by TRITC	Fluorescent microscopy		
<i>Yersinia pestis</i>	Fluorescent probe (RBP proteins from <i>Y. pestis</i> phages ϕ A1122 and L-413C)	Fluorescent microscopy	-	[63]
<i>Campylobacter jejuni</i> , <i>Campylobacter coli</i>	Microresonator functionalized with the GST-Gp48 tailspike	Biosensors	-	[64]
	RBP and GFP-coupled RBP (Gp047)	Agglutination assay on glass slide and fluorescent microscopy	-	[65]
<i>Salmonella</i> spp.	TSP-coated gold/incubation in solution	SEM or SPR	10^3 CFU/mL in case of SPR	[66]
	Det7T loaded to the gold-coated surfaces of a CM5 chip	SPR	5×10^7 CFU/mL	[67]
	Metal beads conjugated with HRP-LTF; incubation in solution	enzyme-linked LTF assay (ELLTA)	10^2 CFU/mL	
<i>Shigella</i> spp.	Sf6TSP cloned with Strep-Tag coated microplate wells	ELISA-like tailspike adsorption assay (ELITA)	10^3 CFU/mL	[68]
<i>Bacillus anthracis</i>	NanoLuc-RBP $_{\lambda 03\Delta 1-120}$, RBP conjugated with commercial luciferase	Enzyme-linked phage receptor binding protein assay (ELPRA)-luminescence	-	[69]
	HRP moiety directly conjugated to the RBP $_{\lambda 03\Delta 1-120}$	ELPRA-colorimetric assay		
<i>Klebsiella pneumoniae</i>	Gp86 RBP fused with mCherry	Fluorescence microscopy and RBP-based fluorescent spectroscopy	-	[70]

Legend: GFP—green fluorescent protein; CFU—colony forming unit; TFP—tail fiber protein; SEM—scanning electron microscopy; SPR—surface plasmon resonance; ELPRA—enzyme-linked phage receptor binding protein assays; FITC—fluorescein isothiocyanate; MALDI-TOF MS—Matrix-Assisted Laser Desorption Ionization–Time of Flight Mass Spectrometry; RBP—receptor binding protein; TSP—tailspike proteins; HRP—horseradish peroxidase.

2.1. *Acinetobacter baumannii* Detection

Acinetobacter baumannii, considered to be one of the opportunistic pathogens, is notorious for its propensity to cause nosocomial infections, including sepsis and ICU (Intensive Care Unit)-acquired pneumonia [71]. It is one of the ESKAPE pathogens, which are a group of highly virulent bacteria with high antimicrobial resistance that are able to “escape” the harmful effects of antibiotics and cause serious infections [72,73]. The success of this pathogen has further been attributed to its outstanding ability to withstand harsh environmental conditions. This is achieved in part through surface glycans such as CPS (capsular polysaccharide), which is composed of multiple repeating oligosaccharide units [74]. The CPS structure called the K type has been elucidated for multiple *A. baumannii* isolates, but no comprehensive serotype classification has been developed to date [75]. The extraordi-

nary diversity of the *A. baumannii* CPS is reflected by the existence of at least 128 different gene clusters (KL clusters) responsible for CPS synthesis and export [76]. Importantly, CPS is targeted by phage RBP during adsorption [77]. Increasing evidence suggests that the K type is an important specificity determinant, with many *A. baumannii* phages infecting strains of a single or very limited number of K types [78–82].

Many groups have studied *A. baumannii* phage tail fiber/tailspike proteins with a particular focus on their depolymerase activity and potential as a prospective antiviral treatment [83–88]. Below, we outline research attempts to harness the specificity of RBPs for detecting *A. baumannii*. The extensive diversity of CPSs in this pathogen limits the feasibility of a method aimed at its rapid and broad-range detection. A more feasible application for phage RBPs in this case might be using them to develop a typing scheme. Xu et al. (2020) recently described the isolation of a new phage capable of infecting five strains of *A. baumannii*. The authors identified two putative tail fiber proteins (TFPs) in genomes of these phages and demonstrated that they bind susceptible cells and lack lytic activity, and thus could be useful as detection tools. To examine the target specificity of the TFPs, the authors devised a sandwich fluorescent assay. Microplate wells were coated with non-labeled TFPs to capture bacterial cells, and bacteria were subsequently detected using analogous, FITC (fluorescein isothiocyanate)-labeled proteins and fluorescence microscopy. The probes exhibited good specificity, as they did not recognize selected strains of *E. coli*, *Acinetobacter haemolyticus* or *Bacillus subtilis*, but they did recognize a susceptible *A. baumannii* strain in a mixed culture. For a detection assay, bacteria were incubated with TFPs conjugated to magnetic beads and the results were visualized using a bioluminescence assay with a commercial luciferin/luciferase kit that measured intracellular ATP release. The authors claimed that an optimized protocol enabled them to detect as few as 6.2×10^2 CFU/mL (colony-forming unit per milliliter) *A. baumannii*. They investigated the clinical applicability of this technique by testing artificially contaminated human samples (urine, sputum, feces), and found that 50–93% of the target bacteria could be recovered from the sample, depending on the sample type and bacterial load [58].

Bai et al. (2019) reported an approach in which alumina-coated magnetic nanoparticles were used to immobilize two distinct TFPs (TF2 and TF6) that selectively recognized two clinical strains of *A. baumannii*. Binding efficiency was evaluated in terms of the change in optical density (OD600) between readouts taken before and after incubation with a nanoparticle probe. The OD change was significantly higher for target bacteria than for non-target bacteria. TEM (transmission electron microscopy) observations showed significant aggregation of nanoparticles, but their binding to bacteria was also apparent.

For the detection of *A. baumannii*, the authors combined nanoparticle trapping with MALDI-TOF MS (matrix-assisted laser desorption-ionization time-of-flight mass spectrometry) analysis to uncover a protein fingerprint for further identification. With this approach, the two *A. baumannii* strains were distinguished from one another as well as from other pathogens (*E. coli* O157:H7 and *Staphylococcus aureus*) in a mixed sample. Additionally, the TFP-coated nanoparticles allowed the sample to be enriched to a concentration of bacteria detectable by MALDI-TOF MS. The level of detection for the method was 2.34×10^5 or 4.48×10^4 CFU/mL, depending on the strain. The method was able to detect low concentrations of bacteria (5×10^5 – 2×10^6 CFU/ml) in diluted fetal bovine serum, supporting its clinical potential. The authors did not examine lower bacterial concentrations, presumably because high ion peaks resulting from the decaying probes would easily obscure the peaks from bacteria present in a sample at a lower concentration. However, MALDI alone, without the selective enrichment, did not detect bacteria present at such a concentration.

To further demonstrate the selectivity of TF2-coated nanoparticles, the authors examined 10 clinical strains: four strains that had been previously described to bind TF2 and six non-binding strains. Bound cells were recovered from the nanoparticles and the CFU of each strain per mg of protein was compared to the value for the original target strain. At a cut-off value established by the authors ($\geq 70\%$ recovery indicating a positive result,

<70% indicating a negative result), TF2-coated nanoparticles could differentiate between known TF2-binding and non-binding strains. [59].

The *A. baumannii* Φ AB6 phage tailspike protein, TF6 (Φ AB6TSP), has attracted attention due to its ability to recognize and hydrolyze bacterial surface glycans containing pseudaminic acid (Pse) [89]. Pse has been identified in numerous Gram-negative pathogens, including *Campylobacter jejuni* and *Helicobacter pylori*, and it has commonly been implicated in virulence [90]. In *A. baumannii* strains, the sequence encoding Pse was identified in two capsule biosynthesis gene clusters [91]. The use of this particular TSP could, in principle, allow the detection of various Pse-coated bacteria. This was recently investigated by Lee et al. (2020). Because the enzymatic activity of Pse could hinder downstream detection, the authors prepared an inactive mutant protein that retained its target specificity. The corresponding inactivated fluorophore-conjugated TSP exhibited a strong relationship between signal intensity and probe/bacterial concentration. The TSP-based probe was deemed to be more sensitive in detecting a susceptible *A. baumannii* strain than an antibody raised against EPS (exopolysaccharide) hydrolysis products containing Pse. The authors also attempted the detection of other Pse-coated bacteria (two strains of *H. pylori* and one of *Enterobacter cloacae*). These strains showed a similar binding capacity, as reflected by fluorescence microscopy observations and the identification of a linear relationship between the fluorescence intensity and optical density of bacterial suspensions. The authors further developed an assay for detecting Pse-coated bacteria by immobilizing the TSP onto the wells of a microplate and measuring the fluorescence of FITC-labeled, bound bacteria. They observed a linear relationship between the amount of bacteria and the fluorescence intensity for Pse-containing strains, but not for Pse-lacking strains. However, the authors noted that the labeling and immobilization steps can introduce significant variation in the results, limiting the usefulness of this technique [60].

2.2. *Campylobacter* spp. Detection

Campylobacter spp. is a Gram-negative foodborne bacterial pathogen. The first report of *Campylobacter* spp. dates back to 1886, when Theodore Escherich observed non-culturable spiral-shaped bacteria. The hosts of this pathogen include both wild and domestic animals; it is frequent among birds, especially poultry, probably because of their higher body temperature [92]. Chicken products have been implicated in a large number of *Campylobacter* spp. infections in human populations, due to the high consumption of chicken meat [93–96]. *Campylobacter* spp. is also commonly found in other livestock, such as cattle, pigs, cows, lambs, ducks, and turkeys [97]. Consumption of untreated water is also considered a risk factor [93,98]. *Campylobacter* spp. causes mild to serious infections of children and the elderly, called campylobacteriosis. The most common symptom is diarrhea, but the infection may lead to permanent neurological damage, such as that of Guillain–Barré syndrome [93]. For *Campylobacter* and certain other species, viable but non-culturable cells (VBNC) can exist (but not replicate) under unfavorable growth conditions. Cells in this state can still infect susceptible hosts [93,99].

Poshtiban et al. (2013) proposed a platform that used the bacteriophage tailspike protein, GST-Gp48, to detect pathogenic *C. jejuni* via an interesting biosensor-based method [64,100]. They employed a micromechanical resonator that enabled the high-throughput and label-free diagnostic analysis of multiple samples. During the experiment, the device monitors the resonance frequency shift, which depends on the mass of the adsorbed target analyte. The microresonator was functionalized with the GST-Gp48 tailspike protein, and the specific capture and detection of *C. jejuni* cells was demonstrated. This microresonator array was highly mass sensitive and had a large surface-to-volume ratio. The detection and quantification of *C. jejuni* cells were confirmed by an SEM (Scanning Electron Microscope). The simulations of resonance behaviors were tested using Finite Element Analysis (FEA). The results of these simulations showed that the frequency shift was determined by the mass of bacteria captured on the microresonator surface. The authors used SEM visualization to calculate the number of bacteria attached to the sensor and found that 225 ± 13 bacteria

bound to a single element on average. The specificity of capture was established by comparing binding between *C. jejuni* and *E. coli* cells (negative control). The findings were promising, and the method seemed to be relatively inexpensive and rapid compared to conventional methods. This microresonator-based biosensor enabled the highly specific detection of bacteria in a sample with a low bacterial load. Moreover, microresonator arrays do not require sample pre-enrichment and the experiments are label-free [64].

Two methods for detecting *C. jejuni* and *Campylobacter coli* were reported by Javed et al. (2013). The authors described a phage RBP-based agglutination assay and a method of GFP-coupled RBP probe detection combined with fluorescence microscopy. First, the team identified an RBP (Gp047) from *C. jejuni* phage NCTC12673 and established that its C-terminal domain was responsible for its specific host recognition. They found that *C. jejuni* NCTC11168 cells mixed with CC-Gp047 formed aggregates within 1 min on a glass slide. The authors confirmed that the observed aggregates were caused by probe binding and not by autoagglutination of bacterial cells. The agglutination test was performed on a wide range of bacterial species (*C. jejuni*, *C. coli*, *Campylobacter lari*, *Campylobacter fetus*, *Campylobacter fetus venerealis*, *Campylobacter concisus*, *Campylobacter upsaliensis*, *H. pylori*, *E. coli*, and *Salmonella enterica*). The results indicated that agglutination also occurred efficiently when the cells were in the VBNC state. To check the robustness of the method under different conditions, different growth media (MH, BHI, LB, and NCZYM) and buffers (phosphate buffer pH 7.4, HEPES buffer pH 7.4, standard saline, Tris-HCl buffer, pH 7.5, and 5% BSA in PBS) were examined. The agglutination results were the same for all tested conditions. The RBP-based agglutination assay showed 100% specificity for both *Campylobacter* species, and 95% and 90% sensitivity for *C. jejuni* and *C. coli*, respectively. Importantly, agglutination tests are rapid and do not require sophisticated equipment (only a simple glass slide) [65].

For the second method, the authors used GFP-fused CC-Gp047 and fluorescence microscopy for detection. Bacterial suspensions (*C. jejuni* NCTC11168, *C. coli* RM2228, and *E. coli* DH5 α) were incubated with the labeled protein and microscopic observations were carried out. *C. jejuni* and *C. coli* showed green fluorescence, indicating the binding of EGFP_CC-Gp047, while *E. coli* DH5a did not. As a follow-up experiment, the authors tested a mixed culture of bacteria containing *C. jejuni* NCTC11168 and *E. coli* DH5a at a cell number ratio of approximately 1:25. Only *C. jejuni* cells (as discerned by characteristic morphology) showed green fluorescence under microscopic observation. The RBP-based probe, EGFP_CC-Gp047, combined with fluorescence microscopy was thus able to detect low numbers of *C. jejuni* and *C. coli* cells in a mixed culture. Both of the introduced methods are simple and specific and can be used for the simultaneous detection of pathogenic *Campylobacter* species [65].

2.3. *Listeria monocytogenes* Detection

Listeria monocytogenes is a major public health concern in the food industry due to its ability to survive the harsh conditions commonly applied in food processing and preservation, such as low temperature, high salt concentration, dehydration, and extreme pH [101]. Infection with *L. monocytogenes*, known as listeriosis, occurs as a result of ingesting contaminated foods; reported outbreaks of listeriosis have been mainly connected to dairy products, meat, fish, fruits, and vegetables [102]. Listeriosis generally presents as gastroenteritis, but in the case of vulnerable individuals (including children, the elderly, pregnant women, and immunocompromised individuals), it poses a threat of sepsis, meningitis, and premature termination of pregnancy [103]. Given the severity of symptoms in the susceptible population and the finding of a lower infectious dose than previously suspected, the U.S. Food and Drug Administration (FDA) adopted a “zero-tolerance policy” for this pathogen in ready-to-eat foods [104]. In contrast, the current EU (European Union) regulations accept a tolerable limit of 100 CFU/g for foods that do not support the growth of *L. monocytogenes* as they enter the market, as well as those that do support the growth of this pathogen over the product’s shelf life [105].

Currently, the detection of *L. monocytogenes* and other *Listeria* spp. in food samples is commonly based on culture methods [101]. As a general rule, one or two enrichment steps (i.e., incubation in a selective liquid medium) are required to enrich the target bacteria to a detectable concentration and inhibit the growth of competing microflora. Cultures are then plated onto selective differential or chromogenic media and the resulting colonies are examined for characteristic morphology. As a slow-growing microorganism, *Listeria* spp. requires extended incubation times, making this a relatively slow process. Thus, new, rapid, and robust detection methods are needed. Numerous nucleic acid-based techniques have been applied to the detection of *L. monocytogenes*, including PCR, multiplex PCR, real time/quantitative PCR (qPCR), loop-mediated isothermal amplification (LAMP), and whole-genome sequencing analyses. For a more detailed description of representative culture methods and novel molecular approaches, the interested reader is referred to the review by Law et al. (2015). These molecular techniques are extremely sensitive and specific; however, they are generally unable to discriminate between viable and inactivated microorganisms, resulting in false positives [106]. Meanwhile, the harsh conditions of food processing are expected to stress bacterial cells, causing them to become non-cultivable on selective media and leading to their underestimation in culture-based methods [107].

L. monocytogenes is currently classified into 12 serotypes; of them, serotypes 1/2a, 1/2b, and 4b are the most commonly associated with clinical disease [108]. The serotypes are determined primarily by the structure of the cell wall-associated carbohydrate polymer, teichoic acid, which is specifically recognized during phage adsorption by RBP [109]. Phages of Gram-positive hosts, including *L. monocytogenes*, possess endolysins (peptidoglycan-cleaving enzymes) with CBDs that exhibit remarkable specificity towards peptidoglycan-associated molecules, including teichoic acid [48,110]. The selectiveness of both types of phage-derived proteins supports their possible application in diagnostic and/or serotyping tools.

The phage-based methods reported to date for detecting *L. monocytogenes* have focused primarily on endolysins [38,49,53,54] and broad-range *Listeria* reporter phages [55,111,112]. A commercially available rapid and semi-automated phage protein-based test for detecting *Listeria* spp. was developed and validated (VIDAS UP *Listeria*, bioMérieux) [112]. Based on the principle of enzyme-linked fluorescent assay, this method uses alkaline phosphatase-conjugated protein probes to capture target bacteria onto a solid surface and direct substrate cleavage to enable fluorescence detection [113]. However, the exact identity of the utilized phage proteins has not been disclosed.

The applicability of phage TFP and endolysins for the diagnosis and typing of *L. monocytogenes* was recently demonstrated by Sumrall et al. (2020). The authors gathered a set of six proteins (three RBP and three endolysin-derived CBD) from a collection of *Listeria* phages with the aim of developing a quick, reliable, and objective serotyping method. In this scheme, GFP-tagged recombinant proteins were incubated with bacteria on a microplate and the fluorescence from bound probes was measured to provide a serovar-specific fingerprint in ~1 h. To verify the accuracy of this novel glycotyping scheme, the authors tested 60 strains of known serotypes; of them, 58 were correctly assigned by the method. Unlike traditional serotyping with a slide agglutination test, which relies on the polyvalent binding of antibodies in serum, this technique relies on precisely described interactions with specific sugar moieties. Importantly, it eliminated the potential discrepancies that could be caused by the subjective interpretation of results or the use of serum preparations from different batches. It also circumvented some of the limitations of PCR-based typing, as it differentiated between live and inactivated bacteria as well as between closely related serotypes arising from a single point mutation.

To further illustrate the usefulness of the phage protein-based detection and differentiation of *L. monocytogenes*, the authors developed a method for differentially separating the most common pathogenic serotypes: 1/2 and 4b. Paramagnetic beads were functionalized with one of two selected GFP-tagged RBPs to allow for the selective enrichment and detection of these serotypes under fluorescence microscopy. The probe-bound beads were found

to be efficient at separating the target serotypes in a mixed culture, although the binding affinity of the 4b-specific beads was significantly lower than that of the 1/2-specific ones. This finding led the authors to develop avidin-tagged directionally coupled probes that exhibited significantly better affinity but lacked the GFP tag essential for fluorescence-based detection. When tested against a comprehensive library of strains of different serotypes, both probes exhibited good specificity. Surprisingly, the 4b-targeting beads also bound nonpathogenic *Listeria innocua* serotype 6a and *L. monocytogenes* 4e, even though the latter harbored few target glycan molecules. These results suggest that phage tail proteins could be a useful tool for developing a rapid and reliable diagnostic assay for *L. monocytogenes* [109].

A different strategy for detecting *Listeria* spp., *E. coli* O157:H7, and *Salmonella* spp. was implemented by Junillon et al. (2012). The authors developed a simple device comprising a polystyrene surface coated with phage proteins and a colorimetric reaction to visualize bound bacteria. The detection was carried out directly in homogenized food samples over the course of a standard enrichment-period incubation (22–40 h depending on the strain) in a liquid medium. The visualization was based on the reduction of colorless triphenyltetrazolium chloride. The resulting red formazan crystals accumulated inside the cells, giving the sensor surface a colored appearance upon binding. To test the applicability of this method, the authors incubated homogenates with approximately 5 CFU of a given strain in the presence of the detection device. The test gave a strong positive result for *L. monocytogenes* serotype 4b and *Listeria seeligeri* in roast pork. Of note, this test used a broad-range phage protein and thus did not discern between different *Listeria* species [114].

2.4. *Yersinia pestis* Detection

Yersinia pestis is a highly pathogenic Gram-negative bacterium that is the causative agent for plague. Historically, this serious and potentially deadly zoonotic disease was responsible for pandemics occurring in the mid-6th, mid-14th, and early 20th centuries [63,115]. *Y. pestis*, which is a member of the *Enterobacteriaceae* family, is a nonmotile, non-spore-forming coccobacillus. Its growth temperature ranges from 4 to 40 °C, with an optimum range of 28–30 °C. The high pathogenicity of this bacterium reflects its ability to adapt to temperature changes: it can survive and replicate in both cold-blooded insects (fleas with body temperature of 20–28 °C) and warm-blooded mammals. Moreover, the bacterium can form a gel-like protective capsule with antiphagocytic properties. Humans can become infected after being bitten by a rodent-hosted flea or by direct contact with animals suffering from plague. Three clinical forms of plague can be distinguished: bubonic, pneumonic, and septicemic. Pneumonic plague is the most serious form of the disease, and the only one that can be transmitted from person to person. Due to its highly contagious nature, *Y. pestis* is currently detected with the following methods: ELISA (enzyme-linked immunosorbent assay)-based antigen detection, culture-based identification, F1 capsule antigen detection, PCR amplification, and virulence gene detection [115]. RBP proteins from *Y. pestis* phages ϕ A1122 and L-413C were coupled to a fluorescent reporter protein to create a specific fluorescent probe for detecting bacterial cells under fluorescence microscopy. The initial observations confirmed that both tested proteins bound to *Y. pestis* cells after only 20 min of incubation. The authors then examined how culture temperature influenced the efficiency of binding. The results indicated that after 2 h incubation with bacteria in early logarithmic phase, RBP binding was observed at all tested temperatures (6, 20, 28, and 37 °C). However, the fluorescent signals for both RBPs were significantly weaker at 6 °C than at higher temperatures (20–37 °C for phage L-413C RBP and 28–37 °C for phage ϕ A1122 RBP) [115]. The specificity of this test was confirmed using *Y. pestis* and other *Yersinia* species as a control, and the assay was performed under different growth and capsule-inducing conditions [115].

2.5. *Pseudomonas aeruginosa* Detection

Pseudomonas aeruginosa is a significant problem in healthcare systems. Infections caused by this bacterium are problematic in ICUs and are associated with high morbidity and mortality. This pathogen is especially dangerous for people with pneumonia, chronic obstructive pulmonary disease, or cystic fibrosis. The World Health Organization put this microorganism on the priority list of bacterial pathogens for which the development of new drugs is urgently needed [116]. This bacterium is responsible for 10–15% of nosocomial infections worldwide [117]. Additionally, infections caused by *Pseudomonas* are difficult to treat due to antibiotic resistance and the ability of this pathogen to acquire resistance to different antimicrobial agents [118]. *P. aeruginosa*-related bloodstream infection, which is considered to be one of its most serious complications, has a mortality of 18–61% [62]. Efforts to develop rapid diagnostic tests for pathogen recognition is an important element of the fight against *P. aeruginosa*-induced infections. One proposed method used a recombinant phage tail fiber protein (P069) from phage PA1. P069 was composed of wild-type TFP, a six-histidine (6-His) tag at the C-terminus, and three lysines at the N-terminus. To confirm the detection of bacteria by interaction of the obtained fluorescent protein, the authors performed TRITC (tetraethyl rhodamine isothiocyanate) labeling. The interaction of *P. aeruginosa* PA1 with the fluorescently labeled protein was observed under fluorescence microscopy. P069 was further functionalized with AffiAmino magnetic particles and incubated with *P. aeruginosa* to show the potential of magnetic separation as a tool for specific bacterial detection. The usefulness of P069 for efficiently detecting *P. aeruginosa* was confirmed in human urine, glucose, and rat serum samples. Together, these P069-based bioluminescent and fluorescent methods detected *P. aeruginosa* with lower limits of 6.7×10^2 CFU/mL and 1.7×10^2 CFU/mL, respectively [119].

2.6. *Enterococcus* spp. and *Staphylococcus* spp. Detection

Staphylococcus aureus is a major human pathogen that causes a wide range of diseases and is the leading cause of healthcare-associated infections [120]. *S. aureus* can colonize healthy individuals: approximately 30% of humans are asymptomatic nasal carriers of this bacterium [121], and *S. aureus* carriers have an increased risk of infection and are presumed to be an important source for the spread of *S. aureus* among individuals [122]. Epidemiological data indicate that the population incidence of bacteremia caused by *S. aureus* ranges from 10 to 30 per 100,000 persons per year [123]. This bacterium is known for its ability to become resistant to antibiotics, and this has become an epidemiological problem on a global scale. Diseases induced by methicillin-resistant *S. aureus* strains (MRSA) often occur in epidemic waves initiated by one or a few successful clones; these waves are problematic in both healthcare and community settings [122,124].

Enterococcus spp. lives harmlessly in the digestive tract, but if it spreads to other parts of the human body, it can cause serious health problems. Hospitals are the most common source of these infections. The use of more intensive and invasive medical therapies for humans has caused enterococcal infections to become more common. Increasing antibiotic resistance has also been noted among clinical isolates of enterococci. Many healthcare-associated strains have become resistant to vancomycin, penicillin, and aminoglycosides. *Enterococcus faecium* is more antibiotic-resistant than *Enterococcus faecalis*; more than half of the pathogenic isolates of the former exhibit resistance to different drugs [125]. Enterococcal infections are often responsible for urinary tract infections among hospitalized patients [126], along with intra-abdominal, pelvic, and soft tissue infections [127], bacteremia [128], and endocarditis [129]. Prompt diagnosis of enterococcal infection is essential for efforts to slow disease progression. One possible strategy is to use the lab-on-chip platform, which offers the benefits of low sample consumption and the possibility for fast and simple analysis [61]. The platform was combined with phage RBPs specific for *Enterococcus* spp. (gp18) and *Staphylococcus* spp. (gp109) for detection of nosocomial pathogens. The utilized proteins had two distinct domains: a C-terminal domain responsible for substrate recognition and receptor binding, and an N-terminal domain engineered

to have a 6-His tag [130]. The N-terminal 6-His tag could form a stable complex with heavy metals, such as nickel, and Ni-magnetic beads were used to enable the oriented attachment of the phage RBP [131]. For analysis, bacterial cells were labeled with magnetic nanoparticles functionalized with specific phage proteins, which recognize phage RBP immobilized at the magnetoresistive chip surface. Finally, the magnetically labeled cells were detected by an array of spin-valve sensors on the biochip. This procedure was reported to take less than 2 h and detect both pathogens at concentrations in the range of 10 CFU/mL [132].

2.7. *Salmonella* spp. Detection

Each year, *Salmonella* infection causes 93.8 million cases of gastroenteritis and 155,000 deaths around the world [133]. It is recognized as the second most common zoonotic pathogen in Europe [134]. *Salmonella enterica* subsp. *enterica* serovar Enteritidis (*S. enteritidis*) and *Salmonella* Typhimurium are responsible for 60% and 30%, respectively, of all reported cases of human salmonellosis in the EU [135]. Members of the genus *Salmonella* belong to the family *Enterobacteriaceae* and are Gram-negative, facultative anaerobic bacilli. The genus is composed of two species, *S. enterica* (with six subspecies) and *Salmonella bongori*, and may be further subdivided into serotypes based on the presence of specific surface molecules, namely H-antigen (H-Ag, typically the major protein of the flagellar complex), flagellin, and O-antigen [136]. Members of *Salmonella* cause a well-characterized spectrum of diseases in humans, ranging from asymptomatic carriage to fatal typhoid fever. In the developed world, foodborne acute gastroenteritis and enterocolitis are the most common forms of *Salmonella* infection [66]. Under stress conditions, cells of *S. Typhimurium* tend to enter a metabolic starvation mode and may remain in a VBNC state. Bacteria in this state cannot be cultivated on conventional culture media but may still show high virulence. Detection of these pathogens has become a major challenge for food safety [137]. All conventional microbiological methods are highly selective and sensitive, but the use of culture-based biochemical and serological assays is time-consuming, laborious, and expensive [138]. The entire process can take at least 5 days to reach a diagnosis [139]. As a promising potential approach, researchers have proposed using biosensors to detect bacterial cells or toxins [67]. The combined use of a biosensor with bacteriophages or their products that can specifically bind *Salmonella* would conceivably be much easier and faster than the conventional methods.

Singh et al. (2010) reported new methods for the sensitive and selective detection of *S. Typhimurium* using genetically engineered TSP from phage P22. In the first such method, TSP mutated to have a cysteine at the N- or C-terminus (to abolish endorhamnosidase activity) were immobilized on a gold substrate. The authors incubated this system with *S. Typhimurium* in liquid medium for 20 min, and then detected bacterial cells with SEM or by fluorescence using SYTO staining. These proteins were more efficient in binding bacteria than whole P22 phage or the corresponding wild-type TSP, most likely due to the lack of enzymatic activity, which can cause cell lysis. Three *E. coli* strains tested to assess selectiveness showed negligible binding and the presence of non-host bacteria with host bacteria did not interfere with the probe activity, supporting the validity of this method. For real-time analytical detection using surface plasmon resonance (SPR), TSP were combined with gold substrate on SF-10 glass plates. Bacteria flowed at 100 $\mu\text{L}/\text{mL}$ for 30 min. A concentration of *S. Typhimurium* as low as 10^3 CFU/mL yielded a significant signal. The presence of an *E. coli* strain did not alter the binding activity for *Salmonella*, confirming the selectiveness of this assay. The mutated TSP further showed resistance to drying with N_2 , whereas whole-phage P22 lost its ability to bind the host bacteria after this process [138].

Hyeon et al. (2021) recently used full-length Det7 phage tail protein (Det7T) in a new SPR-based method for the rapid and selective detection of *S. Typhimurium* [140]. Det7T exhibited 50% sequence identity to the tail endorhamnosidase of *Podovirus* P22 [141], and both of these proteins bound octasaccharide fragments from *Salmonella* LPS. In addition to its strong infection ability, Det7T offered the potential for binding additional *Salmonella* serovars, exhibiting a combined susceptibility of approximately 60% across all *Salmonella*

strains [142]. The developed biosensor system was composed of Det7T loaded to the gold-coated surfaces of a CM5 chip. Binding kinetics were observed for up to 5×10^7 CFU/mL of *Salmonella*. This system exhibited no binding to non-host *E. coli* K12 cells. On SPR, the Det7T signal intensities were 10 times higher than those obtained with mutated P22 tailspike protein [138].

Hyeon et al. (2021) further examined the applicability of this biosensor by testing it against 10% apple juice spiked with *S. Typhimurium* cells. A notable signal was obtained across 5×10 to 5×10^7 CFU/mL. The low detection sensitivity observed in this experiment most likely reflected that oligosaccharide fragments in juice could compete with sensor binding sites. The addition of a pretreatment step that removes additional saccharides might increase the accuracy of this method. Nonetheless, the reported results indicate that a biosensor with Det7T could be a useful tool for the rapid and selective monitoring of *S. Typhimurium* in environmental and food samples.

LTFs such as those from phage S16 have also been used for the rapid and specific immobilization and detection of *S. Typhimurium*. Denyes et al. (2017) used a gp-37 and gp-38 protein complex in combination with metal beads. After the conditions were optimized, the authors tested their system against various concentrations of *S. Typhimurium* DB7155 (from 10 to 10^5 CFU/mL). The results showed that the level of recovery was 98%. Comparison of nine additional strains of *Salmonella* and several monophasic *S. Typhimurium* isolates revealed that the LTF-metal beads could recover 81–97% of the cells. In contrast, less than 5% recovery was observed for *E. coli* K12, *Citrobacter freundii*, *Cronobacter sakazakii* (which have similar Gram-negative structures) and *S. Typhimurium* DB7155 without LTF. The recovery ability for *S. Typhimurium* was not affected by the use of a mixture of different foodborne pathogens. The LTF-metal beads also proved useful in recovering *S. Typhimurium* DB7155 mixed with six food samples (milk, chocolate milk, RIF (reference infant formula), chicken, celery, alfalfa sprouts) at concentrations of 0, 1 to 10, 10, 100, and 1000 CFU per 25 mL or g. *Salmonella* CFU were detected in all samples containing at least 10 CFU/25 g or mL. In chicken, RIF, chocolate milk, and milk, contamination was detected at 1 to 10 CFU/25 g or mL. In terms of the USDA (United States Department of Agriculture) Microbiology Laboratory Guidebook and the FDA Bacteriological Analytical Manual, these results meet the required detection limit for *Salmonella* [139,143] while reducing the detection time from 72 h to 24 h in comparison with the current culture-based methods.

Denyes et al. (2017) further introduced an enzyme-linked LTF assay (ELLTA) that used LTF conjugated with horseradish peroxidase (HRP-LTF). This conjugate was coated onto the metal beads, which were incubated with *Salmonella* cells for 30 min. The unbound HRP-LTF was removed and a buffer containing 3,3', 5,5'-tetramethylbenzidine (TMB) was added. This caused *Salmonella*-containing samples to turn visibly blue. To verify the sensitivity of this test, the authors tested bacterial dilutions from 10 to 10^8 CFU/mL of *S. Typhimurium* DB7155 and used LTF-metal beads incubated with no cells and empty beads as controls. Bacteria-free controls exhibited a negligible amount of TMB (assessed by absorbance at 450 nm; A450). ELLTA was found to be sensitive, yielding significant results against as little as 10^2 CFU/mL. The limit of detection for the reliable and practical detection of *Salmonella* was determined to be 0.49 A450, such that a sample with a value greater than 0.49 A450 was considered to be positive for *Salmonella*. The authors further tested the possibility of using ELLTA to rapidly count *Salmonella* cells. Indeed, measurement of A450 values for dilutions of 10 to 10^8 CFU/mL *S. Typhimurium* DB7155 revealed a linear relationship of log₁₀ CFU/mL to A450 readings between 10^5 and 10^7 CFU/mL, suggesting that this method could be appropriate for counting *Salmonella* cells within this concentration range [135].

Finally, the authors tested the specificity of ELLTA at a concentration of 10^5 CFU/mL. Cross-genus *Salmonella* strains from food and clinical isolates, including five monophasic *S. Typhimurium* strains that are difficult to identify using routine tests and 10 non-*Salmonella* bacteria (Gram-positive and -negative), were checked. The results revealed that all of the *Salmonella* strains could be detected at values ranging from 0.62 to 3.02 A450. The 10 non-*Salmonella* strains had values below the level of detection. A detection efficiency score was

determined by dividing the A450 value by the initial cell number, enabling the authors to rank the individual strains by the detection ability of HRP-LTF. All of the non-*Salmonella* strains had negative or near-zero detection efficiencies. The observed fluctuations in the ability of these strains to interact with HRP-LTF resulted from differences in the structure of cell surface [135].

In sum, this method could detect *S. Typhimurium* at concentrations from 10^2 CFU/mL as well as 20 other *Salmonella* strains in just 2 h [135]. In comparison, conventional culture-based detection takes 5–7 days [143] and requires higher cell concentrations.

2.8. *Shigella* Detection

Humans represent the natural reservoir of *Shigella* spp., but increasing numbers of resistant strains are also found in livestock farming [144]. As *Shigella* is transmitted by the fecal–oral route, most cases of foodborne disease are associated with poor hygiene in food processing and preparation, especially in developing countries. Outbreaks commonly occur when food is exposed to a limited heat treatment or served/delivered raw to the consumer. Food products from which *Shigella* has been isolated include potato salad, ground beef, bean dip, raw oysters, fish, and raw vegetables [145].

The genus *Shigella* comprises four named species: *Shigella dysenteriae* (15 serotypes), *Shigella flexneri* (8 serotypes), *Shigella boydii* (18 serotypes), and *Shigella sonnei* (1 serotype). These four strains do not produce flagellins or capsular antigens and are subdivided into serotypes based on their O-antigens [146]. *S. flexneri* serotype 2a is the most prominent in developing countries [68]. *Shigella* is closely related to *E. coli* (EIEC) (enteroinvasive *E. coli*), complicating the design of a method to correctly detect the cause of an infection. Typical symptoms of *Shigella* infection include bloody diarrhea, abdominal pain, fever, and malaise [145]. Importantly, *S. flexneri* can cause an infection at only 10 CFU/mL, which is below the limit of detection for the current detection methods. The efficient detection of *Shigella* is therefore limited by the time needed to apply bacterial enrichment [147].

Various standardized methods have been developed to isolate and identify *Shigella* spp. from food samples. Some are included in the Bacteriological Analytical Manual (BAM) of the US FDA. Sf6 is a *Podovirus* phage for which *S. flexneri* serotype Y is a host. The tailspike protein from phage Sf6 (Sf6TSP) shows highly specific binding to a polysaccharide on the surface of this bacterium and has been used to develop methods for identifying *S. flexneri* [148]. Although Sf6TSP is an adhesin, it also exhibits enzymatic properties: it can act as an endorhamnosidase, cleaving α -(1→3) linkages between two rhamnoses. The authors used these properties to develop two methods involving Sf6TSP and reported that their engineered Sf6TSP could: (1) be applied in a rapid microtiter plate-based assay; and (2) be used as a sensitive fluorescent probe to enable detection.

Given the high specificity of Sf6TSP, the authors first tested whether it could be a suitable probe for *S. flexneri* in an ELISA-like tailspike adsorption assay (ELITA). For this purpose, they cloned an enzymatically inactivated Sf6TSP E366A/D399A carrying an N-terminal Strep-tag[®]II (StrepII-Sf6TSP). This was tested against four strains of *S. flexneri* and control strains of *E. coli* and *S. Typhimurium*. Bacteria were grown to stationary phase and adsorbed to the surface of a plate coated with StrepII-Sf6TSP. For detection of the modified protein, the authors used HRP-Strep-Tactin[®]. Positive identification was obtained for all four tested strains of *S. flexneri*, whereas no signal was obtained for *E. coli* or *S. Typhimurium*. As a reference control, the authors used P22TSP, which is a TSP known to bind *S. Typhimurium*. Tests performed using Sf6TSP showed results comparable to those obtained with P22TSP. The efficiency in the proposed *Shigella* detection method turned out to be higher or comparable to that used for the detection of *Salmonella*, depending on the *S. flexneri* strain [148,149]. To confirm that the O-antigen is responsible for the binding of the bacterium with the phage adhesin, the authors first incubated the bacteria with an enzymatically active Sf6TSP to remove the bacterial O-antigen. When ELISA was performed with Sf6TSP-treated bacterial cells, the obtained signals were reduced to 24–62% of those obtained with the non-pretreated cells, depending on the *S. flexneri* strain. To

assess the serotype specificity of Sf6TSP, the authors added a Y polysaccharide preparation to the ELITA, setting up competition between the cell-surface O-antigen and free O-antigen polysaccharides in the solution. The Sf6TSP probe was quenched by the free antigens and could not bind to the bacterial surface. The results obtained showed that ELITA-based detection of *S. flexneri* was an exclusively O-antigen-specific process and the TSP did not bind to any other part of the target bacterium.

Kunstmann et al. (2018) also reported a fluorescent detection method for *S. flexneri*. For this purpose, the authors designed a specific Sf6TSP probe in which labeling with the environment-sensitive dye, N-methyl-N-[2-[methyl(7-nitro-2,1,3-benzoxadiazol-4-yl)amino]ethyl] (NBD), was used to generate a signal only upon O-antigen binding. The Sf6TSP probe was coupled with NBD via cysteine residues. When the labeled protein complex bound to the bacterial cell, fluorescence emission was increased as expected [150]. Kunstmann et al. (2018) found that the binding rate of the modified protein did not differ from that of the unlabeled protein, suggesting that this method could be applicable for detecting the *S. flexneri* O-antigen.

2.9. *Bacillus anthracis* Detection

Bacillus anthracis is an etiological factor of anthrax. It is a worldwide zoonosis caused by a Gram-positive, spore-forming bacterium. Infections in humans are caused by contact with animals, particularly grazing herbivores, and with animal products such as wool. Anthrax takes one of three forms [151,152], and the most common infection type is cutaneous anthrax; this form occurs in about 90% of cases. The other two forms are gastrointestinal and pulmonary anthrax [151]. *B. anthracis* is a dangerous pathogen and is considered to be a biological weapon. For this reason, a rapid detection method should be developed. The gold standard for *B. anthracis* testing is still the PCR method, which targets genetic markers (dhp61, PL3, plcR). For rapid pathogen detection, e.g., in the field, lateral flow assays (LFAs) are used. Unfortunately, this method does not seem to be highly sensitive or specific [69].

Braun et al. (2021) proposed a *B. anthracis* detection method based on phages RBPs. The authors developed two enzyme-linked phage RBP assays called ELPRA. Both tests were based on BA4079 protein (named RBP λ_{03}) encoded by lambdoid prophage 03 located on the chromosome of *B. anthracis*. The N-terminally truncated version of the protein (RBP $\lambda_{03\Delta 1-120}$) was also proposed, which was shown to bind specifically to *B. anthracis* cells in different growth phases. The first presented method was the Colony Lift and Blot ELPRA—in this method, the authors grew overnight bacterial cultures on agar plates; next, the colonies were blotted onto hydrophobic nitrocellulose membranes. To detect bacterial colonies, NanoLuc-RBP $\lambda_{03\Delta 1-120}$, RBP conjugated with commercial luciferase, was used (NanoLuc from Promega). To confirm the binding of the modified protein on the membrane of the bacterial cells, Nano-Glo[®] Luciferase Assay Substrate from Promega was used and luminescence was recorded on a ChemiDoc MP imaging system. Researchers used this assay to detect colonies of *B. anthracis* in a mixed culture plate with *B. cereus* and were able to distinguish *B. cereus* from *B. anthracis* as only the colonies of *B. anthracis* exhibited luminescence due to specific binding of NanoLuc-RBP $\lambda_{03\Delta 1-120}$. In addition, a spiked soil sample was tested to identify *B. anthracis* in a heterogeneous environmental culture and the results were promising: only *B. anthracis* colonies were detected, with only one strain of *Bacillus* resulting in a false positive. As stated by the authors, if the process is started at the colony lift step, the assay takes about 1.5–2 h [69].

The second method was called the Rapid Dichotomous Colorimetric ELPRA. For this assay, the authors prepared two protocols: a two-step, indirect ELPRA and a one-step direct ELPRA. In the two-step ELPRA, RBPs fused with mCherry and TwinStrepTag (TST) were used. First, the colonies from agar plate were lifted with a loop and resuspended in the PBS in test tube, and following several washing steps, Strep-Tactin[®]/horseradish peroxidase conjugate was added to the samples. For detection, SeramunBlau[®]/slow peroxidase substrate (containing 3,3',5,5'-tetramethylbenzidin) was used and the development of a blue signal

was monitored [69]. This was relatively fast since the assay, which includes the wash steps, could be completed under 30 min. In the one-step version of this method, the HRP moiety was directly conjugated to the RBP $_{\lambda 03\Delta 1-120}$ reporter protein. When HRP-RBP $_{\lambda 03\Delta 1-120}$ was tested on *B. anthracis* and *B. cereus* colony material, only *B. anthracis* yielded blue signals.

The two presented procedures for *B. anthracis* detection, the colony lift and blot ELPRA, have potential to be a novel tool for rapid pathogen identification. The ELPRA implementation linking the RBP has the potential to be a rapid colorimetric method for specific bacteria detection, supporting PCR-based testing. The specificity of this procedure is high with an overall specificity of >95%. Together with the possibility of obtaining the result in a few minutes, this means that these protocols can be used in rapid diagnostic testing.

2.10. *Klebsiella pneumoniae* Detection

Klebsiella pneumoniae is a well-known multidrug-resistant pathogen and has been declared a global concern of top priority. According to the European Centre for Disease Prevention and Control (ECDC) report from 2019, *Klebsiella* spp. Strains were among the three strains that most often caused pneumonia in patients undergoing intensive care [153,154]. In addition, a report from the World Health Organization (WHO) indicates that approx. 50% of detected *K. pneumoniae* strains are multidrug-resistant [155,156]. Time-consuming and mainly culture-based methods are primarily used to detect infection caused by this pathogen. It is known that infection with this pathogen leads to rapidly progressing pneumonia and sepsis. Therefore, promising *K. pneumoniae* infection detection tools are phages and phage-derived proteins.

Nogueira et al., 2021 reported new isolated *Klebsiella* phage KpnM6E1. The authors also identified and characterized a novel RBP gp86. First, gp86 fused with mCherry was produced. Next, specificity and selectivity of protein binding to the cells were studied by epifluorescence microscopy. The presented results suggested that gp86 RBP was specific for *K. pneumoniae*, and red fluorescence was observed only for this strain. To confirm the binding of the protein, RBP-based fluorescence spectroscopy was used. This method was recently developed by the group for multiplex detection of *Staphylococcus* and *Enterococcus* [129]. The obtained results supported the data collected from the microscopy assays. For other species tested, such as *Staphylococcus* spp., *A. baumannii*, *Enterococcus* spp., or *P. aeruginosa*, no fluorescence was detected. The sensitivity of this test was high, and RBP was able to recognize 80% of *K. pneumoniae* strains [70].

As the authors suggested, the novel RBP presented in Nogueira et al. 2021 provided a sensitive and specific biorecognition molecule for *K. pneumoniae* detection. As presented in this paper, RBP was fused with a fluorescence tag which allowed for the use of the RBP in fluorescence microscopy, ELISA, or spectrofluorometry. Additionally, gp86 can be used in other biosensor assays, for example, SPR, surface-enhanced Raman scattering (SERS), label-free long period gratings (LPGs), or microwave sensors [70].

3. Conclusions

Bacteriophages combine several properties that are desirable for the purpose of detecting bacterial pathogens. In this review, the authors focused on capture-dependent methods in which phage tail proteins are used to detect pathogenic bacteria. The reviewed methods include numerous examples in which phage RBPs are used to rapidly and specifically detect hosts. The described methods include colorimetric, fluorescent, SPR, and microscopy-based detection strategies. Compared to the traditional culture-based methodologies, capture-dependent methodologies are accurate, reliable, simple, relatively inexpensive, fast, and require a fairly low skill level. These properties are all desirable for diagnostics, suggesting that phage tail protein-based capture methods could potentially improve the treatment and control of pathogenic bacteria, thereby decreasing their negative impact worldwide.

Author Contributions: Conceptualization, K.F. and E.B.; writing—original draft preparation, K.F.; *A. baumannii* and *L. monocytogenes* writing part, S.O.; *Salmonella* and *Shigella* writing part, J.B.; *P. aeruginosa*, *Enterococcus* and *Staphylococcus* writing part, B.S.-O.; *Campylobacter* and *Y. pestis* writing part, K.F.; *B. anthracis* and *K. pneumoniae* writing part, KF; writing—review and editing, K.F., B.S.-O., S.O., E.B.; visualization, K.F.; supervision, K.F., E.B.; funding acquisition, E.B. All authors have read and agreed to the published version of the manuscript.

Funding: This research was funded by National Science Center, Poland (Grant Numbers UMO-2017/26/E/NZ1/00249).

Institutional Review Board Statement: Not applicable.

Informed Consent Statement: Not applicable.

Data Availability Statement: Not applicable.

Conflicts of Interest: The authors declare no conflict of interest.

References

1. Ackerman, H.W. 5500 Phages examined in the electron microscope. *Arch. Virol.* **2007**, *152*, 227–243. [[CrossRef](#)] [[PubMed](#)]
2. Jończyk, E.; Kłak, M.; Międzybrodzki, R.; Górski, A. The influence of external factors on bacteriophages—Review. *Folia Microbiol.* **2011**, *56*, 191–200. [[CrossRef](#)] [[PubMed](#)]
3. Weinbauer, M.G. Ecology of prokaryotic viruses. *FEMS Microbiol. Rev.* **2004**, *28*, 127–181. [[CrossRef](#)]
4. Slopek, S.; Przondo-Hessek, H.; Milch, H.; Deák, S. A working scheme for bacteriophage typing of *Klebsiella bacilli*. *Arch. Immunol. Ther. Exp.* **1967**, *15*, 589–599.
5. Abdelsattar, A.S.; Dawooud, A.; Rezk, N.; Makky, S.; Safwat, A.; Richards, P.J.; El-Shibiny, A. How to Train Your Phage: The Recent Efforts in Phage Training. *Biologics* **2021**, *1*, 70–88. [[CrossRef](#)]
6. Stone, E.; Campbell, K.; Grant, I.; McAuli, O. Understanding and Exploiting Phage–Host Interactions. *Viruses* **2019**, *11*, 567. [[CrossRef](#)]
7. Fernandes, S.; São-José, C. Enzymes and Mechanisms Employed by Tailed Bacteriophages to Breach the Bacterial Cell Barriers. *Viruses* **2018**, *10*, 396. [[CrossRef](#)]
8. Pyra, A.; Brzozowska, E.; Pawlik, K.; Gamian, A.; Dauter, M.; Dauter, Z. Tail tubular protein A: A dual function tail protein of *Klebsiella pneumoniae* bacteriophage KP32. *Sci. Rep.* **2017**, *7*, 2223. [[CrossRef](#)]
9. Pyra, A.; Filik, K.; Szermer-Olearnik, B.; Czarny, A.; Brzozowska, E. New Insights on the Feature and Function of Tail Tubular Protein B and Tail Fiber Protein of the Lytic Bacteriophage YeO3-12 Specific for *Yersinia enterocolitica* Serotype O:3. *Molecules* **2020**, *25*, 4392. [[CrossRef](#)]
10. Kutter, E.; Sulakvelidze, A. *Bacteriophages: Biology and Applications*; CRC Press: Washington, DC, USA, 2004.
11. Echeverría-Vega, A.; Morales-Vicencio, P.; Saez-Saavedra, C.; Alvarez, M.A.; Gordillo, F.; Del-Valle, R.; Solís, M.E.; Araya, R. Characterization of the Bacteriophage vB_VorS-PVo5 Infection on *Vibrio ordalii*: A Model for Phage-Bacteria Adsorption in Aquatic Environments. *Front. Microbiol.* **2020**, *11*, 2440. [[CrossRef](#)]
12. Yin, J.; McCaskill, J.S. Replication of viruses in a growing plaque: A reaction-diffusion model. *J. Biophys. Soc.* **1992**, *61*, 1540–1549. [[CrossRef](#)]
13. Brzozowska, E.; Bazan, J.; Gamian, A. The function of bacteriophage proteins. *Postepy Hig. Med. Dosw. (Online)* **2011**, *65*, 167–176. [[CrossRef](#)] [[PubMed](#)]
14. Adams, M.H. *Bacteriophages with Chapters*; Anderson, E.S., Gots, J.S., Jacob, F., Wollman, E.L., Eds.; Interscience Publishers, Inc.: New York, NY, USA, 1959; Volume 5, p. xviii + 592.
15. Szermer-Olearnik, B.; Drab, M.; Małkosa, M.; Zembala, M.; Barbasz, J.; Dąbrowska, K.; Boratyński, J. Aggregation/dispersion transitions of T4 phage triggered by environmental ion availability. *J. Nanobiotechnol.* **2017**, *15*, 32. [[CrossRef](#)] [[PubMed](#)]
16. Philippe, C.; Chaïb, A.; Jaomanjaka, F.; Cluzet, S.; Lagarde, A.; Ballestra, P.; Decendit, A.; Petrel, M.; Claisse, O.; Goulet, A.; et al. Wine Phenolic Compounds Differently Affect the Host-Killing Activity of Two Lytic Bacteriophages Infecting the Lactic Acid Bacterium *Oenococcus oeni*. *Viruses* **2020**, *12*, 1316. [[CrossRef](#)] [[PubMed](#)]
17. Delbrück, M. Biochemical mutants of bacterial viruses. *J. Bacteriol.* **1948**, *56*, 1–16. [[CrossRef](#)]
18. Ackermann, H.W. Tailed bacteriophages: The order Caudovirales. In *Advances in Virus Research*; Academic Press: Cambridge, MA, USA, 1999; Volume 51, pp. 135–201. [[CrossRef](#)]
19. Molineux, I.J. T7-LIKE PHAGES (PODOVIRIDAE). In *Encyclopedia of Virology*, 2nd ed.; Granoff, A., Webster, R.G., Eds.; Elsevier: Amsterdam, The Netherlands, 1999; pp. 1722–1729.
20. Mosig, G. T4-LIKE PHAGES (MYOVIRIDAE). In *Encyclopedia of Virology*, 2nd ed.; Granoff, A., Webster, R.G., Eds.; Elsevier: Amsterdam, The Netherlands, 1999; pp. 1706–1716.
21. Aksyuk, A.A.; Leiman, P.G.; Kurochkina, L.P.; Shneider, M.M.; Kostyuchenko, V.A.; Mesyanzhinov, V.V.; Rossmann, M.G. The tail sheath structure of bacteriophage T4: A molecular machine for infecting bacteria. *EMBO J.* **2009**, *28*, 821–829. [[CrossRef](#)]

22. Leiman, P.G.; Arisaka, F.; Van Raaij, M.J.; Kostyuchenko, V.A.; Aksyuk, A.A.; Kanamaru, S.; Rossmann, M.G. Morphogenesis of the T4 tail and tail fibers. *Viol. J.* **2010**, *7*, 355. [[CrossRef](#)]
23. Tao, Y.; Strelkov, S.V.; Mesyanzhinov, V.V.; Rossmann, M.G. Structure of bacteriophage T4 fibrin: A segmented coiled coil and the role of the C-terminal domain. *Structure* **1997**, *5*, 789–798. [[CrossRef](#)]
24. Bartual, S.G.; Otero, J.M.; Garcia-Doval, C.; Llamas-Saiz, A.L.; Kahn, R.; Fox, G.C.; van Raaij, M.J. Structure of the bacteriophage T4 long tail fiber receptor-binding tip. *Proc. Natl. Acad. Sci. USA* **2010**, *107*, 20287–20292. [[CrossRef](#)]
25. Campbell, A.M. Coliphage Lambda (Siphoviridae). In *Encyclopedia of Virology*, 2nd ed.; Granoff, A., Webster, R.G., Eds.; Elsevier: Amsterdam, The Netherlands, 1999; pp. 281–285.
26. Simpson, D.J.; Sacher, J.C.; Szymanski, C.M. Development of an assay for the identification of receptor binding proteins from bacteriophages. *Viruses* **2016**, *8*, 17. [[CrossRef](#)] [[PubMed](#)]
27. Meile, S.; Kilcher, S.; Loessner, M.J.; Dunne, M. Reporter Phage-Based Detection of Bacterial Pathogens: Design Guidelines and Recent Developments. *Viruses* **2020**, *12*, 944. [[CrossRef](#)] [[PubMed](#)]
28. Singh, A.; Arutyunov, D.; Szymanski, C.M.; Evoy, S. Bacteriophage based probes for pathogen detection. *Analyst* **2012**, *137*, 3405. [[CrossRef](#)] [[PubMed](#)]
29. Singh, A.; Poshtiban, S.; Evoy, S. Recent advances in bacteriophage based biosensors for food-borne pathogen detection. *Sensors* **2013**, *13*, 1763–1786. [[CrossRef](#)]
30. Gao, J.; Jeffries, L.; Mach, K.E.; Craft, D.W.; Thomas, N.J.; Gau, V.; Liao, J.C.; Wong, P.K. A Multiplex Electrochemical Biosensor for Bloodstream Infection Diagnosis. *SLAS Technol.* **2017**, *22*, 466–474. [[CrossRef](#)]
31. Vásquez, G.; Rey, A.; Rivera, C.; Iregui, C.; Orozco, J. Amperometric biosensor based on a single antibody of dual function for rapid detection of *Streptococcus agalactiae*. *Biosens. Bioelectron.* **2017**, *87*, 453–458. [[CrossRef](#)]
32. Spehar-Délèze, A.M.; Julich, S.; Gransee, R.; Tomaso, H.; Dulay, S.B.; O’Sullivan, C.K. Electrochemiluminescence (ECL) immunosensor for detection of *Francisella tularensis* on screen-printed gold electrode array. *Anal. Bioanal. Chem.* **2016**, *408*, 7147–7153. [[CrossRef](#)]
33. Farooq, U.; Ullah, M.W.; Yang, Q.; Aziz, A.; Xu, J.; Zhou, L.; Wang, S. High-density phage particles immobilization in surface-modified bacterial cellulose for ultra-sensitive and selective electrochemical detection of *Staphylococcus aureus*. *Biosens. Bioelectron.* **2020**, *157*, 112163. [[CrossRef](#)]
34. Singh, A.; Arutyunov, D.; McDermott, M.T.; Szymanski, C.M.; Evoy, S. Specific detection of *Campylobacter jejuni* using the bacteriophage NCTC 12673 receptor binding protein as a probe. *Analyst* **2011**, *136*, 4780. [[CrossRef](#)]
35. Peng, H.; Chen, I.A. Rapid Colorimetric Detection of Bacterial Species through the Capture of Gold Nanoparticles by Chimeric Phages. *ACS Nano* **2019**, *13*, 1244–1252. [[CrossRef](#)]
36. Kong, M.; Sim, J.; Kang, T.; Nguyen, H.H.; Park, H.K.; Chung, B.H.; Ryu, S. A novel and highly specific phage endolysin cell wall binding domain for detection of *Bacillus cereus*. *Eur. Biophys. J.* **2015**, *44*, 437–446. [[CrossRef](#)] [[PubMed](#)]
37. Tolba, M.; Ahmed, M.U.; Tlili, C.; Eichenseher, F.; Loessner, M.J.; Zourob, M. A bacteriophage endolysin-based electrochemical impedance biosensor for the rapid detection of *Listeria* cells. *Analyst* **2012**, *137*, 5749–5756. [[CrossRef](#)] [[PubMed](#)]
38. Le Brun, G.; Hauwaert, M.; Leprince, A.; Glinel, K.; Mahillon, J.; Raskin, J.P. Electrical Characterization of Cellulose-Based Membranes towards Pathogen Detection in Water. *Biosensors* **2021**, *11*, 57. [[CrossRef](#)] [[PubMed](#)]
39. Wang, J.; McIvor, M.J.; Elliott, C.T.; Karoonuthaisiri, N.; Segatori, L.; Biswal, S.L. Rapid detection of pathogenic bacteria and screening of phage-derived peptides using microcantilevers. *Anal. Chem.* **2014**, *86*, 1671–1678. [[CrossRef](#)]
40. Liu, P.; Han, L.; Wang, F.; Petrenko, V.A.; Liu, A. Gold nanoprobe functionalized with specific fusion protein selection from phage display and its application in rapid, selective and sensitive colorimetric biosensing of *Staphylococcus aureus*. *Biosens. Bioelectron.* **2016**, *82*, 195–203. [[CrossRef](#)]
41. Farooq, U.; Yang, Q.; Ullah, M.W.; Wang, S. Bacterial biosensing: Recent advances in phage-based bioassays and biosensors. *Biosens. Bioelectron.* **2018**, *118*, 204–216. [[CrossRef](#)] [[PubMed](#)]
42. Anany, H.; Chou, Y.; Cucic, S.; Derda, R.; Evoy, S.; Griffiths, M.W. From Bits and Pieces to Whole Phage to Nanomachines: Pathogen Detection Using Bacteriophages. *Annu. Rev. Food Sci. Technol.* **2017**, *8*, 305–329. [[CrossRef](#)] [[PubMed](#)]
43. Gerstmans, H.; Criel, B.; Briers, Y. Synthetic biology of modular endolysins. *Biotechnol. Adv.* **2018**, *36*, 624–640. [[CrossRef](#)]
44. Loessner, M.J.; Kramer, K.; Ebel, F.; Scherer, S. C-terminal domains of *Listeria monocytogenes* bacteriophage murein hydrolases determine specific recognition and high-affinity binding to bacterial cell wall carbohydrates. *Mol. Microbiol.* **2002**, *44*, 335–349. [[CrossRef](#)]
45. Maciejewska, B.; Olszak, T.; Drulis-Kawa, Z. Applications of bacteriophages versus phage enzymes to combat and cure bacterial infections: An ambitious and also a realistic application? *Appl. Microbiol. Biotechnol.* **2018**, *102*, 2563–2581. [[CrossRef](#)]
46. Oliveira, H.; Melo, L.D.; Santos, S.B.; Nóbrega, F.L.; Ferreira, E.C.; Cerca, N.; Azeredo, J.; Kluskens, L.D. Molecular aspects and comparative genomics of bacteriophage endolysins. *J. Virol.* **2013**, *87*, 4558–4570. [[CrossRef](#)] [[PubMed](#)]
47. Mo, K.F.; Li, X.; Li, H.; Low, L.Y.; Quinn, C.P.; Boons, G.J. Endolysins of *Bacillus anthracis* bacteriophages recognize unique carbohydrate epitopes of vegetative cell wall polysaccharides with high affinity and selectivity. *J. Am. Chem. Soc.* **2012**, *134*, 15556–15562. [[CrossRef](#)] [[PubMed](#)]
48. Dams, D.; Briers, Y. Enzybiotics: Enzyme-Based Antibacterials as Therapeutics. In *Therapeutic Enzymes: Function and Clinical Implications. Advances in Experimental Medicine and Biology*; Labrou, N., Ed.; Springer: Singapore, 2019; Volume 1148. [[CrossRef](#)]

49. Schmelcher, M.; Shabarova, T.; Eugster, M.R.; Eichenseher, F.; Tchang, V.S.; Banz, M.; Loessner, M.J. Rapid multiplex detection and differentiation of *Listeria* cells by use of fluorescent phage endolysin cell wall binding domains. *Appl. Environ. Microbiol.* **2010**, *76*, 5745–5756. [CrossRef] [PubMed]
50. Cho, J.H.; Kwon, J.G.; O'Sullivan, D.J.; Ryu, S.; Lee, J.H. Development of an endolysin enzyme and its cell wall-binding domain protein and their applications for biocontrol and rapid detection of *Clostridium perfringens* in food. *Food Chem.* **2021**, *345*, 128562. [CrossRef]
51. Gómez-Torres, N.; Dunne, M.; Garde, S.; Meijers, R.; Narbad, A.; Ávila, M.; Mayer, M.J. Development of a specific fluorescent phage endolysin for in situ detection of *Clostridium* species associated with cheese spoilage. *Microb. Biotechnol.* **2018**, *11*, 332–345. [CrossRef]
52. Chang, Y.; Ryu, S. Characterization of a novel cell wall binding domain-containing *Staphylococcus aureus* endolysin LysSA97. *Appl. Microbiol. Biotechnol.* **2016**, *101*, 147–158. [CrossRef]
53. Walcher, G.; Stessl, B.; Wagner, M.; Eichenseher, F.; Loessner, M.J.; Hein, I. Evaluation of paramagnetic beads coated with recombinant *Listeria* phage endolysin-derived cell-wall-binding domain proteins for separation of *Listeria monocytogenes* from raw milk in combination with culture-based and real-time polymerase chain reaction-based quantification. *Foodborne Pathog. Dis.* **2010**, *7*, 1019–1024. [CrossRef]
54. Kretzer, J.W.; Lehmann, R.; Schmelcher, M.; Banz, M.; Kim, K.P.; Korn, C.; Loessner, M.J. Use of high-affinity cell wall-binding domains of bacteriophage endolysins for immobilization and separation of bacterial cells. *Appl. Environ. Microbiol.* **2007**, *73*, 1992–2000. [CrossRef]
55. Kretzer, J.W.; Schmelcher, M.; Loessner, M.J. Ultrasensitive and Fast Diagnostics of Viable *Listeria* Cells by CBD Magnetic Separation Combined with A511::luxAB Detection. *Viruses* **2018**, *10*, 626. [CrossRef]
56. Park, C.; Kong, M.; Lee, J.H.; Ryu, S.; Park, S. Detection of *Bacillus cereus* using bioluminescence assay with cell wall-binding domain conjugated magnetic nanoparticles. *BioChip J.* **2018**, *12*, 287–293. [CrossRef]
57. Kong, M.; Shin, J.H.; Heu, S.; Park, J.K.; Ryu, S. Lateral flow assay-based bacterial detection using engineered cell wall binding domains of a phage endolysin. *Biosens. Bioelectron.* **2017**, *96*, 173–177. [CrossRef] [PubMed]
58. Xu, J.; Li, X.; Kang, G.; Bai, L.; Wang, P.; Huang, H. Isolation and Characterization of AbTJ, an *Acinetobacter baumannii* Phage, and Functional Identification of Its Receptor-Binding Modules. *Viruses* **2020**, *12*, 205. [CrossRef] [PubMed]
59. Bai, Y.L.; Shahed-Al-Mahmud, M.; Selvaprakash, K.; Lin, N.T.; Chen, Y.C. Tail Fiber Protein-Immobilized Magnetic Nanoparticle-Based Affinity Approaches for Detection of *Acinetobacter baumannii*. *Anal. Chem.* **2019**, *91*, 10335–10342. [CrossRef] [PubMed]
60. Lee, I.M.; Tu, I.F.; Yang, F.L.; Wu, S.H. Bacteriophage Tail-Spike Proteins Enable Detection of Pseudaminic-Acid-Coated Pathogenic Bacteria and Guide the Development of Antiglycan Antibodies with Cross-Species Antibacterial Activity. *J. Am. Chem. Soc.* **2020**, *142*, 19446–19450. [CrossRef]
61. Murdoch, D.R.; Corey, G.R.; Hoen, B.; Miró, J.M.; Fowler, V.G., Jr.; Bayer, A.S.; Karchmer, A.W.; Olaison, L.; Pappas, P.A.; Moreillon, P.; et al. International Collaboration on Endocarditis-Prospective Cohort Study (ICE-PCS) Investigators. Clinical presentation, etiology, and outcome of infective endocarditis in the 21st century: The International Collaboration on Endocarditis-Prospective Cohort Study. *Arch. Intern. Med.* **2009**, *169*, 463–473. [CrossRef]
62. Vidal, F.; Mensa, J.; Almela, M.; Martinez, J.A.; Marco, F.; Casals, C.; Gatell, J.M.; Soriano, E.; de Jimenez Anta, M.T. Epidemiology and outcome of *Pseudomonas aeruginosa* bacteremia, with special emphasis on the influence of antibiotic treatment. Analysis of 189 episodes. *Arch. Intern. Med.* **1996**, *156*, 2121–2126. [CrossRef]
63. Perry, R.D.; Fetherston, J.D. *Yersinia pestis*—etiologic agent of plague. *Clin. Microbiol. Rev.* **1997**, *10*, 35–66. [CrossRef]
64. Poshtiban, S.; Singh, A.; Fitzpatrick, G.; Evoy, S. Bacteriophage tail-spike protein derivitized microresonator arrays for specific detection of pathogenic bacteria. *Sens. Actuators B Chem.* **2013**, *181*, 410–416. [CrossRef]
65. Javed, M.A.; Poshtiban, S.; Arutyunov, D.; Evoy, S.; Szymanski, C.M. Bacteriophage receptor binding protein based assays for the simultaneous detection of *Campylobacter jejuni* and *Campylobacter coli*. *PLoS ONE* **2013**, *8*, e69770. [CrossRef]
66. Denyes, J.M.; Dunne, M.; Steiner, S.; Mittelviehhaus, M.; Weiss, A.; Schmidt, H.; Klumpp, J.; Loessner, M.J. Modified bacteriophage S16 long tail fiber proteins for rapid and specific immobilization and detection of *Salmonella* cells. *Appl. Environ. Microbiol.* **2017**, *83*, e00277-17. [CrossRef]
67. Andrews, W.H.; Jacobson, A.; Hammack, T. “Bacteriological Analytical Manual (BAM) Chapter 5: *Salmonella*”. Bacteriological Analytical Manual (2018).* Bacteriological Analytical Manual Chapter 5: *Salmonella*. Available online: <https://www.fda.gov/food/laboratory-methods-food/bam-chapter-5-salmonella> (accessed on 26 September 2021).
68. Coimbra, R.S.; Grimont, F.; Grimont, P.A. Identification of *Shigella* serotypes by restriction of amplified O-antigen gene cluster. *Res. Microbiol.* **1999**, *150*, 543–553. [CrossRef]
69. Braun, P.; Rupprich, N.; Neif, D.; Grass, G. Enzyme-Linked Phage Receptor Binding Protein Assays (ELPRA) Enable Identification of *Bacillus anthracis* Colonies. *Viruses* **2021**, *13*, 1462. [CrossRef] [PubMed]
70. Nogueira, C.L.; Pires, D.P.; Monteiro, R.; Santos, S.B.; Carvalho, C.M. Exploitation of a *Klebsiella* Bacteriophage Receptor-Binding Protein as a Superior Biorecognition Molecule. *ACS Infect. Dis.* **2021**, *7*, 3077–3087. [CrossRef] [PubMed]
71. Garnacho-Montero, J.; Timsit, J.F. Managing *Acinetobacter baumannii* infections. *Curr. Opin. Infect. Dis.* **2019**, *32*, 69–76. [CrossRef]
72. Mulani, M.S.; Kamble, E.E.; Kumkar, S.N.; Tawre, M.S.; Pardesi, K.R. Emerging Strategies to Combat ESKAPE Pathogens in the Era of Antimicrobial Resistance: A Review. *Front. Microbiol.* **2019**, *10*, 539. [CrossRef]

73. Rice, L.B. Federal funding for the study of antimicrobial resistance in nosocomial pathogens: No ESKAPE. *J. Infect. Dis.* **2008**, *197*, 1079–1081. [[CrossRef](#)]
74. Harding, C.M.; Hennon, S.W.; Feldman, M.F. Uncovering the mechanisms of *Acinetobacter baumannii* virulence. *Nat. Rev. Microbiol.* **2018**, *16*, 91–102. [[CrossRef](#)]
75. Shashkov, A.S.; Kenyon, J.J.; Arbatsky, N.P.; Shneider, M.M.; Popova, A.V.; Miroshnikov, K.A.; Volozhantsev, N.V.; Knirel, Y.A. Structures of three different neutral polysaccharides of *Acinetobacter baumannii*, NIPH190, NIPH201, and NIPH615, assigned to K30, K45, and K48 capsule types, respectively, based on capsule biosynthesis gene clusters. *Carbohydr. Res.* **2015**, *417*, 81–88. [[CrossRef](#)]
76. Wyres, K.L.; Cahill, S.M.; Holt, K.E.; Hall, R.M.; Kenyon, J.J. Identification of *Acinetobacter baumannii* loci for capsular polysaccharide (KL) and lipooligosaccharide outer core (OCL) synthesis in genome assemblies using curated reference databases compatible with Kaptive. *Microb. Genom.* **2020**, *6*, e000339. [[CrossRef](#)]
77. Gordillo Altamirano, F.; Forsyth, J.H.; Patwa, R.; Kostoulias, X.; Trim, M.; Subedi, D.; Archer, S.K.; Morris, F.C.; Oliveira, C.; Kiely, L.; et al. Bacteriophage-resistant *Acinetobacter baumannii* are resensitized to antimicrobials. *Nat. Microbiol.* **2021**, *6*, 157–161. [[CrossRef](#)]
78. Shchurova, A.S.; Shneider, M.M.; Arbatsky, N.P.; Shashkov, A.S.; Chizhov, A.O.; Skryabin, Y.P.; Mikhaylova, Y.V.; Sokolova, O.S.; Shelenkova, A.A.; Miroshnikov, K.A.; et al. Novel *Acinetobacter baumannii* Myovirus TaPaz Encoding Two Tailspike Depolymerases: Characterization and Host-Recognition Strategy. *Viruses* **2021**, *13*, 978. [[CrossRef](#)] [[PubMed](#)]
79. Popova, A.V.; Lavysh, D.G.; Klimuk, E.I.; Edelstein, M.V.; Bogun, A.G.; Shneider, M.M.; Goncharov, A.E.; Leonov, S.V.; Severin, K.V. Novel Fri1-like Viruses Infecting *Acinetobacter baumannii*-vB_AbaP_AS11 and vB_AbaP_AS12-Characterization, Comparative Genomic Analysis, and Host-Recognition Strategy. *Viruses* **2017**, *9*, 188. [[CrossRef](#)] [[PubMed](#)]
80. Popova, A.V.; Shneider, M.M.; Myakinina, V.P.; Bannov, V.A.; Edelstein, M.V.; Rubalskii, E.O.; Aleshkin, A.V.; Fursova, N.K.; Volozhantsev, N.V. Characterization of myophage AM24 infecting *Acinetobacter baumannii* of the K9 capsular type. *Arch. Virol.* **2019**, *164*, 1493–1497. [[CrossRef](#)]
81. Popova, A.V.; Shneider, M.M.; Arbatsky, N.P.; Kasimova, A.A.; Senchenkova, S.N.; Shashkov, A.S.; Dmitrenok, A.S.; Chizhov, A.O.; Mikhailova, Y.V.; Shagin, D.A.; et al. Specific Interaction of Novel Friunavirus Phages Encoding Tailspike Depolymerases with Corresponding *Acinetobacter baumannii* Capsular Types. *J. Virol.* **2020**, *95*, e01714–20. [[CrossRef](#)] [[PubMed](#)]
82. Oliveira, H.; Costa, A.R.; Konstantinides, N.; Ferreira, A.; Akturk, E.; Sillankorva, S.; Nemeč, A.; Shneider, M.; Dötsch, A.; Azeredo, J. Ability of phages to infect *Acinetobacter calcoaceticus*-*Acinetobacter baumannii* complex species through acquisition of different pectate lyase depolymerase domains. *Environ. Microbiol.* **2017**, *19*, 5060–5077. [[CrossRef](#)]
83. Hernandez-Morales, A.C.; Lessor, L.L.; Wood, T.L.; Migl, D.; Mijalis, E.M.; Cahill, J.; Russell, W.K.; Young, R.F.; Gill, J.J. Genomic and Biochemical Characterization of *Acinetobacter* Podophage Petty Reveals a Novel Lysis Mechanism and Tail-Associated Depolymerase Activity. *J. Virol.* **2018**, *92*, e01064–17. [[CrossRef](#)]
84. Liu, Y.; Mi, Z.; Mi, L.; Huang, Y.; Li, P.; Liu, H.; Yuan, X.; Niu, W.; Jiang, N.; Bai, C.; et al. Identification and characterization of capsule depolymerase Dpo48 from *Acinetobacter baumannii* phage IME200. *PeerJ* **2019**, *7*, e6173. [[CrossRef](#)] [[PubMed](#)]
85. Liu, Y.; Leung, S.; Guo, Y.; Zhao, L.; Jiang, N.; Mi, L.; Li, P.; Wang, C.; Qin, Y.; Mi, Z.; et al. The Capsule Depolymerase Dpo48 Rescues *Galleria mellonella* and Mice from *Acinetobacter baumannii* Systemic Infections. *Front. Microbiol.* **2019**, *10*, 545. [[CrossRef](#)]
86. Shahed-Al-Mahmud, M.; Roy, R.; Sugiokto, F.G.; Islam, M.N.; Lin, M.D.; Lin, L.C.; Lin, N.T. Phage ϕ AB6-Borne Depolymerase Combats *Acinetobacter baumannii* Biofilm Formation and Infection. *Antibiotics* **2021**, *10*, 279. [[CrossRef](#)]
87. Wang, C.; Li, P.; Zhu, Y.; Huang, Y.; Gao, M.; Yuan, X.; Niu, W.; Liu, H.; Fan, H.; Qin, Y.; et al. Identification of a Novel *Acinetobacter baumannii* Phage-Derived Depolymerase and Its Therapeutic Application in Mice. *Front. Microbiol.* **2020**, *11*, 1407. [[CrossRef](#)]
88. Oliveira, H.; Costa, A.R.; Ferreira, A.; Konstantinides, N.; Santos, S.B.; Boon, M.; Noben, J.P.; Lavigne, R.; Azeredo, J. Functional Analysis and Antivirulence Properties of a New Depolymerase from a Myovirus That Infects *Acinetobacter baumannii* Capsule K45. *J. Virol.* **2019**, *93*, e01163–18. [[CrossRef](#)] [[PubMed](#)]
89. Lee, I.M.; Tu, I.F.; Yang, F.L.; Ko, T.P.; Liao, J.H.; Lin, N.T.; Wu, C.Y.; Ren, C.T.; Wang, A.H.; Chang, C.M.; et al. Structural basis for fragmenting the exopolysaccharide of *Acinetobacter baumannii* by bacteriophage Φ AB6 tailspike protein. *Sci. Rep.* **2017**, *7*, 42711. [[CrossRef](#)] [[PubMed](#)]
90. Zunk, M.; Kiefel, M. The occurrence and biological significance of the α -keto-sugars pseudaminic acid and legionaminic acid within pathogenic bacteria. *RSC Adv.* **2014**, *4*, 3413–3421. [[CrossRef](#)]
91. Kenyon, J.J.; Marzaioli, A.M.; De Castro, C.; Hall, R.M. 5,7-di-N-acetyl-acinetaminic acid: A novel non-2-ulosonic acid found in the capsule of an *Acinetobacter baumannii* isolate. *Glycobiology* **2015**, *25*, 644–654. [[CrossRef](#)]
92. Skirrow, M.B. *Campylobacter enteritis: A “new” disease.* *Br. Med. J.* **1997**, *2*, 9. [[CrossRef](#)] [[PubMed](#)]
93. Silva, J.; Leite, D.; Fernandes, M.; Mena, C.; Gibbs, P.A.; Teixeira, P. *Campylobacter* spp. as a foodborne pathogen: A review. *Front. Microbiol.* **2011**, *2*, 200. [[CrossRef](#)]
94. Tauxe, R.V. “Epidemiology of *Campylobacter jejuni* infection in the United States and other industrialized nations,” Chapter 2. In *Campylobacter jejuni: Current Status and Future Trends*; Nachamkin, I., Blaser, M.J., Tompkins, L.S., Eds.; American Association of Microbiologists: Washington, DC, USA, 1992; pp. 9–19.

95. Skirrow, M.B. Campylobacteriosis. In *Zoonoses*; Palmer, S.R., Lord Soulsby, S.R., Simpson, D.I.H., Eds.; Oxford University Press: New York, NY, USA, 1998; pp. 37–46.
96. Corry, J.E.L.; Atabay, H.I. Poultry as a source of Campylobacter and related organisms. *J. Appl. Microbiol.* **2001**, *90*, 96S–114S. [[CrossRef](#)]
97. Humphrey, T.; O'Brien, S.; Madsen, M. Campylobacters as zoonotic pathogens: A food production perspective. *Int. J. Food Microbiol.* **2007**, *117*, 237–257. [[CrossRef](#)]
98. Eberhart-Phillips, J.; Walker, N.; Garrett, N.; Bell, D.; Sinclair, D.; Rainger, W.; Bates, M. Campylobacteriosis in New Zealand: Results of a case-control study. *J. Epidemiol. Community Health* **1997**, *51*, 686–691. [[CrossRef](#)]
99. Portner, D.C.; Leuschner, R.G.K.; Murray, B.S. Optimising the viability during storage of freeze-dried cell preparations of Campylobacter jejuni. *Cryobiology* **2007**, *54*, 265–270. [[CrossRef](#)]
100. Montagut, Y.; Garcia, J.; Jiménez, Y.; March, C.; Montoya, Á.; Arnau, A. QCM technology in biosensors. In *Biosensors-Emerging Materials and Application*; Serra, P.A., Ed.; IntechOpen: London, UK, 2011; pp. 153–178. [[CrossRef](#)]
101. Law, J.W.; Ab Mutalib, N.S.; Chan, K.G.; Lee, L.H. An insight into the isolation, enumeration, and molecular detection of Listeria monocytogenes in food. *Front. Microbiol.* **2015**, *6*, 1227. [[CrossRef](#)] [[PubMed](#)]
102. Schlech, W.F. Epidemiology and Clinical Manifestations of Listeria monocytogenes Infection. *Microbiol. Spectr.* **2019**, *7*. [[CrossRef](#)] [[PubMed](#)]
103. Radoshevich, L.; Cossart, P. Listeria monocytogenes: Towards a complete picture of its physiology and pathogenesis. *Nat. Rev. Microbiol.* **2018**, *16*, 32–46. [[CrossRef](#)] [[PubMed](#)]
104. Archer, D.L. The evolution of FDA's policy on Listeria monocytogenes in ready-to-eat foods in the United States. *Curr. Opin. Food Sci.* **2018**, *20*, 64–68. [[CrossRef](#)]
105. COMMISSION REGULATION (EC) No 2073/2005 of 15 November 2005 on Microbiological Criteria for Foodstuffs. Available online: <https://eur-lex.europa.eu/eli/reg/2005/2073> (accessed on 9 February 2022).
106. Jadhav, S.; Bhave, M.; Palombo, E.A. Methods used for the detection and subtyping of Listeria monocytogenes. *J. Microbiol. Methods* **2012**, *88*, 327–341. [[CrossRef](#)]
107. Bernardo, R.; Duarte, A.; Tavares, L.; Barreto, A.S.; Henriques, A.R. Listeria monocytogenes Assessment in a Ready-to-Eat Salad Shelf-Life Study Using Conventional Culture-Based Methods, Genetic Profiling, and Propidium Monoazide Quantitative PCR. *Foods* **2021**, *10*, 235. [[CrossRef](#)]
108. Datta, A.R.; Burall, L.S. Serotype to genotype: The changing landscape of listeriosis outbreak investigations. *Food Microbiol.* **2018**, *75*, 18–27. [[CrossRef](#)]
109. Sumrall, E.T.; Röhrig, C.; Hupfeld, M.; Selvakumar, L.; Du, J.; Dunne, M.; Schmelcher, M.; Shen, Y.; Loessner, M.J. Glycotyping and Specific Separation of Listeria monocytogenes with a Novel Bacteriophage Protein Tool Kit. *Appl. Environ. Microbiol.* **2020**, *86*, e00612-20. [[CrossRef](#)]
110. Bhagwat, A.; Mixon, M.; Collins, C.H.; Dordick, J.S. Opportunities for broadening the application of cell wall lytic enzymes. *Appl. Microbiol. Biotechnol.* **2020**, *104*, 9019–9040. [[CrossRef](#)]
111. Hagens, S.; de Wouters, T.; Vollenweider, P.; Loessner, M.J. Reporter bacteriophage A511::celB transduces a hyperthermostable glycosidase from Pyrococcus furiosus for rapid and simple detection of viable Listeria cells. *Bacteriophage* **2011**, *1*, 143–151. [[CrossRef](#)]
112. Crowley, E.; Bird, P.; Flannery, J.; Benzinger, M.J., Jr.; Fisher, K.; Boyle, M.; Huffman, T.; Bastin, B.; Bedinghaus, P.; Judd, W.; et al. Evaluation of VIDAS[®] UP Listeria assay (LPT) for the detection of Listeria in a variety of foods and environmental surfaces: First Action 2013.10. *J. AOAC Int.* **2014**, *97*, 431–441. [[CrossRef](#)] [[PubMed](#)]
113. VIDAS[®], L. Monocytogenes Xpress (LMX) Ultra Performance Summary. Available online: https://www.biomerieux-usa.com/sites/subsidiary_us/files/vidas_l_monocytogenes_xpress_8.5x11_v4.pdf (accessed on 9 February 2022).
114. Junillon, T.; Vimont, A.; Mosticone, D.; Mallen, B.; Baril, F.; Rozand, C.; Flandrois, J.P. Simplified detection of food-borne pathogens: An in situ high affinity capture and staining concept. *J. Microbiol. Methods* **2012**, *91*, 501–505. [[CrossRef](#)] [[PubMed](#)]
115. Born, F.; Braun, P.; Scholz, H.C.; Grass, G. Specific detection of yersinia pestis based on receptor binding proteins of phages. *Pathogens* **2020**, *9*, 611. [[CrossRef](#)] [[PubMed](#)]
116. Jurado-Martín, I.; Sainz-Mejías, M.; McClean, S. Pseudomonas aeruginosa: An Audacious Pathogen with Adaptable Arsenal of Virulence Factors. *Int. J. Mol. Sci.* **2021**, *22*, 3128. [[CrossRef](#)] [[PubMed](#)]
117. Blanc, D.S.; Petignat, C.; Janin, B.; Bille, J.; Francioli, P. Frequency and molecular diversity of Pseudomonas aeruginosa upon admission and during hospitalization: A prospective epidemiologic study. *Clin. Microbiol. Infect.* **1998**, *4*, 242–247. [[CrossRef](#)] [[PubMed](#)]
118. Strateva, T.; Yordanov, D. Pseudomonas aeruginosa—A phenomenon of bacterial resistance. *J. Med. Microbiol.* **2009**, *58*, 1133–1148. [[CrossRef](#)]
119. He, Y.; Shi, Y.; Liu, M.; Wang, Y.; Wang, L.; Lu, S.; Fu, Z. Nonlytic Recombinant Phage Tail Fiber Protein for Specific Recognition of Pseudomonas aeruginosa. *Anal. Chem.* **2018**, *90*, 14462–14468. [[CrossRef](#)]
120. Tong, S.Y.C.; Davis, J.S.; Eichenberger, E.; Holland, T.L.; Fowler, V.G., Jr. Staphylococcus aureus Infections: Epidemiology, Pathophysiology, Clinical Manifestations, and Management. *Clin. Microbiol. Rev.* **2015**, *28*, 603–661. [[CrossRef](#)]
121. Kluytmans, J.; van Belkum, A.; Verbrugh, H. Nasal carriage of Staphylococcus aureus: Epidemiology underlying mechanisms, and associated risks. *Clin. Microbiol. Rev.* **1997**, *10*, 505–520. [[CrossRef](#)]

122. Chambers, H.F.; DeLeo, F.R. Waves of Resistance: Staphylococcus aureus in the Antibiotic Era. *Nat. Rev. Microbiol.* **2009**, *7*, 629–641. [[CrossRef](#)]
123. Laupland, K.B.; Lyytikäinen, O.; Søgaard, M.; Kennedy, K.J.; Knudsen, J.D.; Ostergaard, C.; Galbraith, J.C.; Valiquette, L.; Jacobsson, G.; Collignon, P.; et al. The changing epidemiology of Staphylococcus aureus bloodstream infection: A multinational population—Based surveillance study. *Clin. Microbiol. Infect.* **2013**, *19*, 465–471. [[CrossRef](#)] [[PubMed](#)]
124. Kaplan, S.L.; Hulten, K.G.; Gonzalez, B.E.; Hammerman, W.A.; Lamberth, L.; Versalovic, J.; Mason, E.O., Jr. Three-year surveillance of community-acquired Staphylococcus aureus infections in children. *Clin. Infect. Dis.* **2005**, *40*, 1785–1791. [[CrossRef](#)] [[PubMed](#)]
125. Liu, P.; Wang, Y.; Han, L.; Cai, Y.; Ren, H.; Ma, T.; Li, X.; Petrenko, V.A.; Liu, A. Colorimetric Assay of Bacterial Pathogens Based on Co₃O₄ Magnetic Nanozymes Conjugated with Specific Fusion Phage Proteins and Magnetophoretic Chromatography. *ACS Appl. Mater. Interfaces* **2020**, *12*, 9090–9097. [[CrossRef](#)]
126. Agudelo Higueta, N.I.; Huycke, M.M. Enterococcal Disease, Epidemiology, and Implications for Treatment. In *Enterococci: From Commensals to Leading Causes of Drug Resistant Infection*; Massachusetts Eye and Ear Infirmary: Boston, MD, USA, 2014; NBK190429.
127. Hall, L.M.; Duke, B.; Urwin, G.; Guiney, M. Epidemiology of Enterococcus faecalis urinary tract infection in a teaching hospital in London, United Kingdom. *J. Clin. Microbiol.* **1992**, *30*, 1953–1957. [[CrossRef](#)] [[PubMed](#)]
128. Noskin, G.A.; Peterson, L.R.; Warren, J.R. Enterococcus faecium and Enterococcus faecalis bacteremia: Acquisition and outcome. *Clin. Infect. Dis.* **1995**, *20*, 296–301. [[CrossRef](#)] [[PubMed](#)]
129. Hidron, A.I.; Edwards, J.R.; Patel, J.; Horan, T.C.; Sievert, D.M.; Pollock, D.A.; Fridkin, S.K. National Healthcare Safety Network Team. NHSN annual update: Antimicrobial-resistant pathogens associated with healthcare-associated infections: Annual summary of data reported to the National Healthcare Safety Network at the Centers for Disease Control and Prevention, 2006–2007. *Infect. Control Hosp. Epidemiol.* **2008**, *29*, 996–1011. [[CrossRef](#)]
130. Foudeh, A.M.; Didar, T.F.; Veres, T.; Tabrizian, M. Microfluidic designs and techniques using lab-on-a-chip devices for pathogen detection for point-of-care diagnostics. *Lab Chip* **2012**, *12*, 3249–3266. [[CrossRef](#)]
131. Santos, S.B.; Cunha, A.P.; Macedo, M.; Nogueira, C.L.; Brandão, A.; Costa, S.P.; Melo, L.D.R.; Azeredo, J.; Carvalho, C.M. Bacteriophage-receptor binding proteins for multiplex detection of Staphylococcus and Enterococcus in blood. *Biotechnol. Bioeng.* **2020**, *117*, 3286–3298. [[CrossRef](#)]
132. Patel, J.D.; O’Carra, R.; Jones, J.; Woodward, J.G.; Mumper, R.J. Preparation and characterization of nickel nanoparticles for binding to his-tag proteins and antigens. *Pharm. Res.* **2007**, *24*, 343–352. [[CrossRef](#)]
133. Cunha, A.P.; Henriques, R.; Cardoso, S.; Freitas, P.P.; Carvalho, C.M. Rapid and multiplex detection of nosocomial pathogens on a phage-based magnetoresistive lab-on-chip platform. *Biotechnol. Bioeng.* **2021**, *118*, 3164–3174. [[CrossRef](#)]
134. Majowicz, S.E.; Musto, J.; Scallan, E.; Angulo, F.J.; Kirk, M.; O’Brien, S.J.; Jones, T.F.; Fazil, A.; Hoekstra, R.M.; for the International Collaboration on Enteric Disease “Burden of Illness” Studies. The global burden of nontyphoidal Salmonella gastroenteritis. *Clin. Infect. Dis.* **2010**, *50*, 882–889. [[CrossRef](#)] [[PubMed](#)]
135. Di Cesare, A.; Losasso, C.; Barco, L.; Eckert, E.M.; Conficoni, D.; Sarasini, G.; Corno, G.; Ricci, A. Diverse distribution of Toxin-Antitoxin II systems in Salmonella enterica serovars. *Sci. Rep.* **2016**, *6*, 28759. [[CrossRef](#)] [[PubMed](#)]
136. Bell, R.L.; Jarvis, K.G.; Ottesen, A.R.; McFarland, M.A.; Brown, E.W. Recent and emerging innovations in Salmonella detection: A food and environmental perspective. *Microb. Biotechnol.* **2016**, *9*, 279–292. [[CrossRef](#)] [[PubMed](#)]
137. Dekker, J.P.; Frank, K.M. Salmonella, Shigella, and yersinia. *Clin. Lab. Med.* **2015**, *35*, 225–246. [[CrossRef](#)] [[PubMed](#)]
138. Priyanka, B.; Patil, R.K.; Dwarakanath, S. A review on detection methods used for foodborne pathogens. *Indian J. Med. Res.* **2016**, *144*, 327. [[CrossRef](#)]
139. Singh, A.; Arya, S.K.; Glass, N.; Hanifi-Moghaddam, P.; Naidoo, R.; Szymanski, C.M.; Tanha, J.; Evoy, S. Bacteriophage tailspike proteins as molecular probes for sensitive and selective bacterial detection. *Biosens. Bioelectron.* **2010**, *26*, 131–138. [[CrossRef](#)]
140. Walter, M.; Fiedler, C.; Grassl, R.; Biebl, M.; Rachel, R.; Hermo-Parrado, X.L.; Llamas-Saiz, A.L.; Seckler, R.; Miller, S.; van Raaij, M.J. Structure of the receptor-binding protein of bacteriophage det7: A podoviral tail spike in a myovirus. *J. Virol.* **2008**, *82*, 2265–2273. [[CrossRef](#)]
141. Lazcka, O.; Del Campo, F.J.; Munoz, F.X. Pathogen detection: A perspective of traditional methods and biosensors. *Biosens. Bioelectron.* **2007**, *22*, 1205–1217. [[CrossRef](#)]
142. Hyeon, S.H.; Lim, W.K.; Shin, H.J. Novel surface plasmon resonance biosensor that uses full-length Det7 phage tail protein for rapid and selective detection of Salmonella enterica serovar Typhimurium. *Biotechnol. Appl. Biochem.* **2021**, *68*, 5–12. [[CrossRef](#)]
143. Edgar, R.H. Evolution of Bacteriophage Host Attachment Using Det7 as a Model. Master’s Thesis, University of Pittsburgh, Pittsburgh, PA, USA, 4 February 2014.
144. Odumeru, J.A.; León-Velarde, C.G. Salmonella detection methods for food and food ingredients. In *Salmonella-A Dangerous Foodborne Pathogen*; In Tec: Rijeka, Croatia, 2012; pp. 373–392.
145. Liang, B.; Roberts, A.P.; Xu, X.; Yang, C.; Yang, X.; Wang, J.; Yi, S.; Li, Y.; Ma, Q.; Wu, F.; et al. Transferable plasmid-borne mcr-1 in a colistin-resistant Shigella flexneri isolate. *Appl. Environ. Microbiol.* **2018**, *84*, e02655-17. [[CrossRef](#)]
146. Warren, B.R.; Parish, M.E.; Schneider, K.R. Shigella as a foodborne pathogen and current methods for detection in food. *Crit. Rev. Food Sci. Nutr.* **2006**, *46*, 551–567. [[CrossRef](#)] [[PubMed](#)]
147. Muthuirulandi Sethuvel, D.P.; Devanga Ragupathi, N.K.; Anandan, S.; Veeraraghavan, B. Update on: Shigella new serogroups/serotypes and their antimicrobial resistance. *Lett. Appl. Microbiol.* **2017**, *64*, 8–18. [[CrossRef](#)] [[PubMed](#)]

148. DuPont, H.L.; Levine, M.M.; Hornick, R.B.; Formal, S.B. Inoculum size in shigellosis and implications for expected mode of transmission. *J. Infect. Dis.* **1989**, *159*, 1126–1128. [[CrossRef](#)]
149. Kunstmann, S.; Scheidt, T.; Buchwald, S.; Helm, A.; Mulard, L.A.; Fruth, A.; Barbirz, S. Bacteriophage Sf6 tailspike protein for detection of *Shigella flexneri* pathogens. *Viruses* **2018**, *10*, 431. [[CrossRef](#)] [[PubMed](#)]
150. Schmidt, A.; Rabsch, W.; Broeker, N.K.; Barbirz, S. Bacteriophage tailspike protein based assay to monitor phase variable glucosylations in *Salmonella* O-antigens. *BMC Microbiol.* **2016**, *16*, 207. [[CrossRef](#)]
151. Spencer, R.C. *Bacillus anthracis*. *J. Clin. Pathol.* **2003**, *56*, 182–187. [[CrossRef](#)]
152. Swartz, M.N. Recognition and management of anthrax—An update. *N. Engl. J. Med.* **2001**, *345*, 1607–1610. [[CrossRef](#)]
153. Salmanov, A.; Litus, V.; Vdovychenko, S.; Litus, O.; Davtian, L.; Ubogov, S.; Bisyuk, Y.; Drozdova, A.; Vlasenko, I. Healthcare-Associated Infections in Intensive Care Units. *Wiad. Lek.* **2019**, *72*, 963–969. [[CrossRef](#)]
154. European Centre for Disease Prevention and Control. *Surveillance of Antimicrobial Resistance in Europe: Annual Report of the European Antimicrobial Resistance Surveillance Network (EARS-Net) 2017*; ECDC: Solna, Sweden, 2018.
155. World Health Organization. *Central Asian and European Surveillance of Antimicrobial Resistance: Annual Report 2019*; World Health Organization: Geneva, Switzerland, 2019.
156. Suetens, C.; Latour, K.; Kärki, T.; Ricchizzi, E.; Kinross, P.; Moro, M.L.; Jans, B.; Hopkins, S.; Hansen, S.; Lyytikäinen, O.; et al. Prevalence of Healthcare-Associated Infections, Estimated Incidence and Composite Antimicrobial Resistance Index in Acute Care Hospitals and Long-Term Care Facilities: Results from Two European Point Prevalence Surveys, 2016 to 2017. *Eurosurveillance* **2018**, *23*, 1800516. [[CrossRef](#)]